Shape-specific Effects of Cerium Oxide Nanoparticles (CNPs) on Macrophage Polarization

by

VISHAL PRABHAKAR RAKSHE

B. Pharm. in Pharmaceutical Sciences, Bombay College of Pharmacy

Submitted to the Graduate Faculty of

School of Pharmacy in partial fulfillment

of the requirements for the degree of

Master of Science

University of Pittsburgh

2018

UNIVERSITY OF PITTSBURGH

SCHOOL OF PHARAMCY

This thesis was presented

by

VISHAL PRABHAKAR RAKSHE

It was defended on

April 9, 2018

and approved by

Dr. Shilpa Sant, Assistant Professor, School of Pharmacy

Dr. Song Li, Professor, School of Pharmacy

Dr. Kerry Empey, Assistant Professor, School of Pharmacy

Thesis Director Advisor: Dr. Shilpa Sant, Assistant Professor, School of Pharmacy

Copyright © by VISHAL PRABHAKAR RAKSHE

2018

Shape-specific Effects of Cerium Oxide Nanoparticles (CNPs) on Macrophage Polarization

Vishal Prabhakar Rakshe, B. Pharm.

University of Pittsburgh, 2018

Immunotherapy is gaining traction in healthcare research where immune activation is central to the therapeutic interventions. The field of immunotherapy is expected to grow at 15% annually and surpass $100 billion by 2022. The mainstay of immunotherapy revolves around monoclonal antibodies, cytokines, immune-modulators, and checkpoint inhibitors. Fast track approval of newer drugs like Keytruda® (Pembrolizumab, Merck) reveals the need and potential of such medications.

Evidence suggests that the activated macrophages by themselves are capable of identifying and alleviating viral infections. Macrophages display remarkable plasticity and change their phenotype in response to environmental cues. These changes give rise to different populations of cells with distinct functions namely M1 and M2. The goal of the current clinical trials involving lipopolysaccharide (LPS) or muramyldipeptide (MDP) or cytokines such as interferon-γ (IFN-γ) and granulocyte-macrophage colony-stimulating factor (GM-CSF) is to activate macrophages as a novel immunotherapeutic approach. However, inability of LPS to be systemically administered without causing toxicity *in vivo* or short duration of action of MDP and IFN-γ due to rapid clearance has limited their transition as effective clinical alternatives.

Cerium oxide NPs (CNPs) are known to mitigate oxidative stress and alter the free radical balance. Some recent studies suggest that microenvironmental factors such as free radicals can affect macrophage polarization. On the other hand, various nanoparticles (NPs) have shown to modulate

macrophage activation by virtue of their shape. However, interplay between NP shape effects and free radical modulating activity on the macrophage polarization is not known. Thus, we hypothesized that the shape specific CNPs can influence the macrophage phenotypes through their dual attributes: free radical modulating ability and their shapes with various aspect ratios.

We used THP-1 human monocyte cell line as an *in vitro* model. THP-1 monocytes were pre-differentiated to M1 and M2 macrophage phenotypes using appropriate stimuli. Measurement of reactive oxygen and nitrogen species provided an early indication that CNP shape and duration of treatment influenced the inflammatory status of the macrophages. Quantification of mRNA levels of selected M1 and M2 markers revealed shape-dependent effect of CNPs on driving macrophage polarization towards a particular phenotype. Isotropic shape such as Sphere CNPs did not show tendency to drive phenotypic changes. However, anisotropic shapes with different aspect ratios such as Cube (1:1) and Rod (21:1) CNPs showcased a high proclivity to induce an inflammatory M1 phenotype. The ability of Cube and Rod CNPs to increase reactive oxygen and nitrogen species and simultaneously drive M1 phenotype evident from gene expression profiles suggested possible link between these two phenomena. We further confirmed link between CNP shape and free radical modulating activity to drive macrophage polarization through pharmacological inhibition of oxygen and nitrogen radicals. Overall, our results suggest that the biophysical characteristics such as shape of NPs play an important role in dictating macrophage polarization and can be exploited to design better delivery systems for drugs targeting macrophages.

Keywords: Cerium oxide, nanomaterial, free radical modulation, macrophage polarization, M1 and M2 phenotype, reactive oxygen species, reactive nitrogen species, macrophage priming, macrophage re-programming

TABLE OF CONTENTS

LIST OF TABLES

LIST OF FIGURES

ACKNOWLEDGEMENTS

I would like to thank the School of Pharmacy, University of Pittsburgh for granting me the opportunity to pursue my graduate studies. I sincerely express gratitude to my advisor Dr. Shilpa Sant for her unwavering guidance and support. I would also like to thank Dr. Vinayak Sant and Dr. Maggie Folan for all their assistance. I express gratitude to our collaborators Dr. Kerry Empey and Jessica Kosanovich from Empey lab for their valuable inputs regarding my research.

I appreciate the opportunity provided by Dr. Vera Donnenberg and Dr. Albert Donnenberg for conducting flow cytometry experiments in their lab at Hillman Cancer Center. I would also like to thank Bosco Popov for training in sample preparation and Dr. Rathod for helping in analyzing flow results. I would like to thank Dr. Robert Gibbs and Dr. Lisa Rohan for access to confocal and fluorescence microscope respectively. I acknowledge the Center for Pharmacogenetics and Center for Biologic Imaging for access to RT-qPCR and transmission electron microscope respectively.

I would like to acknowledge the overwhelming contributions of Akhil Patel, Yingfei Xue, Dr. Manjulata Singh, Sricharani Balmuri, Yohann Pitale, Qiaoke Gong, Meng-Ni Ho and other members of Sant lab. I want to thank Lori Altenbaugh for her kindest support. I express gratitude to all the faculty, staff and friends from the School of Pharmacy.

I owe deepest gratitude to my parents, brother, Ishwari, uncle and aunt whose constant faith and support motivate me daily to achieve the best.

-------------------------------------Intentionally left blank---

1.0 INTRODUCTION

1.1 Macrophages: Origin and Functions

The body's innate immune system plays a central role in mediating the host's defense against foreign pathogens[1]. The innate arm of immunity concerns itself with the non-specific yet primary response on initial contact with invading pathogens. Innate immunity is comprised of epithelial membranes acting as a physical barrier to the entry of pathogens, actively phagocytic leukocytes such as neutrophils and macrophages, natural killer (NK) cells and a complement system of plasma proteins. Macrophage contribution in the overall scheme of immune cascade is central for a robust immune response. Touted as the primary scavenger cells of the immune system, macrophages boast a unique ability to engulf foreign entities, cellular debris and stressed cells in order to maintain cellular homeostasis as well as carry out immune surveillance. Macrophages are a crucial bridging component between the innate and adaptive immune arms of our defense system. As one of the most effective cell types involved in the emergency response following injury or pathogenic insult, macrophages modulate host defense, inflammatory processes and tissue repair[2]. Armed with formidable abilities of cell engulfment or phagocytosis, antigen processing, antigen presentation, chemokine and cytokine production and subsequent T lymphocyte priming, macrophages govern the initiation and resolution stages of innate and adaptive immunity[3]. The pivotal role of macrophages in the host immunity is primarily due to their plasticity.

Macrophages are derived from the monocytic lineage precursor cells located in the bone marrow. Monocytes are recruited from the circulating blood as and when required. During development and throughout their lifetime, macrophages reside in many tissues of the body and show great functional diversity. They may have specialized function based on their location and distinct gene expression profile. For example, osteoclasts are bone-residing macrophages involved in bone resorption while spleen macrophages perform heme degradation and iron re-cycling[3, 4]. Although tissue macrophages are anatomically distinct from one another, and have different transcriptional profiles and functional capabilities, they are all required for the maintenance of homeostasis[3]. Several attempts have been made to date to classify this versatile and heterogeneous group of cells, the most adopted system being the mononuclear phagocytic system (MPS). The MPS system encompasses these professional phagocytic cells and their bone marrow progenitors[3]. Another type of binary classification accounts for the differential inflammatory status maintained by these different types of macrophages and categorizes them in to two extreme states. This classification includes the classically activated, pro-inflammatory M1 cells and alternately activated, anti-inflammatory M2 cells[3].

Resting or undifferentiated macrophages (M0) adjust to the changes in the residing milieu. This dynamic process of change in macrophage phenotype is defined as ‘macrophage polarization’. The two main activation states are termed as M1 and M2 phenotypes. The phenotype of the polarized macrophages is tightly linked to the microenvironment within which they reside[5]. Various local environmental stimuli such as certain inflammatory mediators and cytokines can potentially modulate the phenotypes[6].

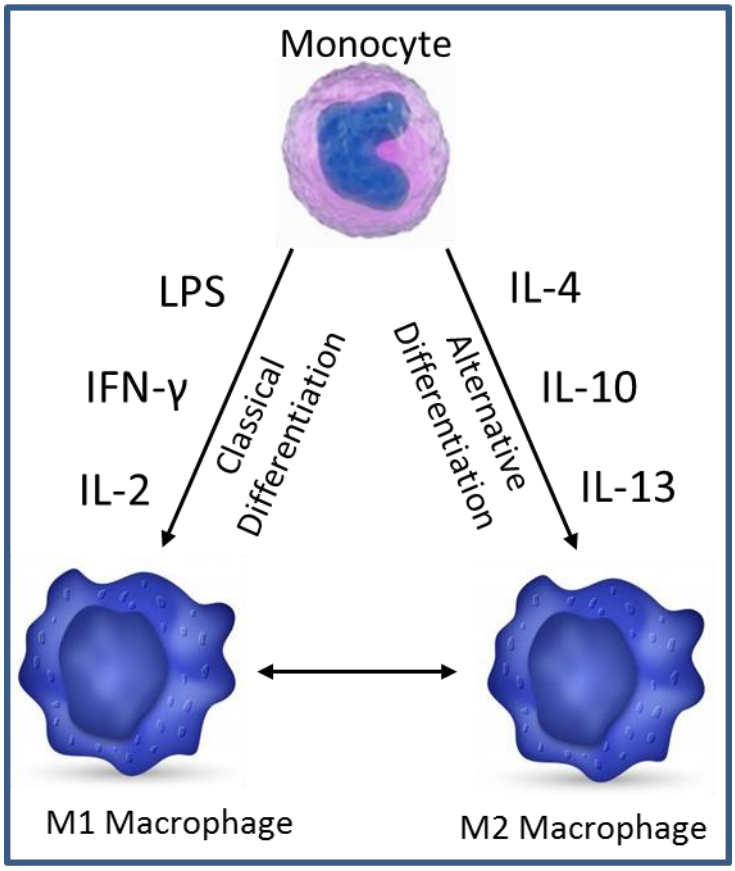

Figure 1: Schematic representing macrophage polarization using cytokine as stimuli

The initiation phase is inundated with the actively phagocytic M1 phenotype to ward off the invading pathogens. M1 phenotype is predominantly responsible for clearance of intracellular pathogens owing to their high phagocytic ability and for release of pro-inflammatory cytokines during the early phase of inflammation in order to recruit and activate T cells and B cells. M1 phenotype is immuno-stimulatory in nature and represents a pro-inflammatory state characterized chiefly by NF-κB activation[7]. In tumorigenesis, M1 macrophages play a protective, anti-tumorigenic role[8]. Thus, M1 macrophages mirror a Th1 response and may also amplify the response. M1 cells are induced *in vitro* by lipopolysaccharide (LPS) and/or interferon- γ (IFN-γ) and characterized by high iNOS, IL-12, TNF-α, IL-1β and a high expression of CD80[9].

During the resolution phase, the predominant phenotype is the anti-inflammatory M2-like phenotype. Characteristic functions of the M2 phenotype include: wound healing, immunosuppression, inducing basement membrane breakdown, angiogenesis, tissue repair, remodeling and other homeostatic functions[9, 10]. M2 macrophages can be induced *in vitro* by treatment with interleukins such as IL-4, IL-10 or IL-13. Based on the stimuli used for M2 induction, they could be further classified into subsets, namely M2a (IL-4/IL-13), M2b (Toll-like Receptor [TLR] agonists), M2c (IL-10). In our discussion, M2 phenotype would be considered as a single entity without dwelling further on to the classification.

Such a binary classification, however, does not do justice to the complex *in vivo* environment for most macrophage types, in which numerous other cytokines and growth factors interact to define the final differentiated state. Transcriptional profiling of resident macrophages by the 'Immunological Genome Project' shows that this population has high transcriptional diversity with minimal overlap, suggesting prevalence of several classes of unique macrophages[11]. However, for the purpose of our discussion, the simplistic binary classification of M1 and M2 macrophages will be used based on the two extremes of macrophage phenotypic behavior. Such a system although overtly simplistic in nature, can determine whether a particular phenotype is involved in the disease state, in nanomaterial uptake and processing and/or its subsequent biological response.

1.2 Macrophage Polarization: Implications in Diseases

The two polarization states of M1 and M2 represent a continuum of the functional spectrum present in dynamic equilibrium[12]. A healthy, uninfected tissue will harbor a mixed M1 and M2 macrophage sub-population. Upon infection the M1 sub-population will increase exponentially to

fight the invading pathogen[10]. Once the infection is cleared, the M2 sub-population will predominate to limit the pro-inflammatory damage to the host tissue as well as initiate wound healing and tissue remodeling[10]. The M1/M2 macrophage balance is maintained by a number of micro-environmental cues such as cytokines, inflammatory mediators, and disease conditions[13]. Many diseased conditions rely on manipulating the macrophage polarization state to advance their progression. On the other hand, presence of macrophages in their 'correct' or desired phenotype can halt or slow disease progression.

M2 macrophages present in tumor tissues have been termed as tumor-associated macrophages (TAMs). Tumor microenvironment preferentially harbors immunosuppressive TAMs that promote tumor progression and malignancy[14]. TAMs stimulate tumor cell migration, invasion and intravasation as well as the angiogenic response essential for metastasis facilitating escape of tumor cells to the circulatory or the lymphatic system[14, 15, 16]. M2 macrophages can prevent development of diet induced obesity and type-2 diabetes by clearing the accumulated cholesterol and are, thus, atheroprotective[17]. M1 macrophages are implicated for many age-associated chronic inflammatory conditions such as rheumatoid arthritis and cardiovascular diseases. Unlike in cancer, the chronic inflammatory conditions do not manipulate macrophage polarization but rely on an immuno-compromised status where the macrophages are not present in the desired phenotype. For instance, absence of IFN-γ or its receptors in mice increases susceptibility to various mycobacterial infection[18, 19]. The presence of a desired phenotype in certain disease conditions has rendered macrophage polarization an attractive target for immunotherapeutic therapies.

1.3 Macrophage Polarization: Modulating Free Radical Balance

The classical approach involves use of cytokine delivery systems to influence the local macrophage population[20]. Cytokines are small, potent proteins capable of affecting the cells around them. The role of cytokines in autocrine, paracrine, endocrine signaling as well as immune-modulating agents has led to their wide spread use as a potential therapeutic approach.

The other micro-environmental cue capable of manipulating macrophage phenotype is the inflammatory status surrounding the cells. Presence of free radicals such as reactive oxygen species (ROS) has been implicated in various pathological disorders, such as cancers, neurodegenerative diseases, infertility, diabetes, cardiovascular diseases, arthritis and aging[21, 22]. Reactive oxygen species include superoxide, peroxides, hydroxyl radical and singlet oxygen. Along with ROS, similar entities such as reactive nitrogen species (RNS) have been associated with these disorders[22]. ROS plays a dual role in cellular physiology[23]. At lower levels, ROS are key players in the signal transduction process acting as secondary messengers in physiological environments. ROS is implicated as a key player mounting antimicrobial and anti-viral defenses[24]. Although no direct evidence of pathogen killing activity of ROS has been established, the free radicals are believed to activate the NF-κB pathway promoting release of interferons[24]. Excessive amounts of ROS and RNS cause oxidative and nitrosative stress respectively, damage macromolecules and lead to cell death through a variety of molecular mechanisms[25]. The environmental cues dictate the macrophage polarization by either of the two mechanisms: priming or activation of naïve macrophages or re-programming of macrophages. In the following sections, we will further explore these two mechanisms as well as the immunotherapeutic approaches that are based on these mechanisms.

1.4 Priming of Macrophages

Many *in vitro* functional and molecular studies involving macrophages often use a single or a combination of two strong polarizing ligands[26]. However *in vivo* macrophages encounter a broad range of stimuli simultaneously whose integration dictates the polarization status of the cells[26]. The priming and activation pathways of these polarizing ligands including LPS, IFN-γ and IL-4 have been well documented[26]. The stimuli required for activation could be broadly classified into two classes, endogenous molecules such as cytokines and danger signals like LPS which are microbial components without a counterpart in humans[1, 27]. These polarizing signals act upon specific surface receptors on the macrophages, initiating a number of signaling pathways and transcription factors followed by modified regulation of gene expression[28]. Three main types of receptor families are involved in macrophage activation based on the major transcription factors coupled to them[28]. Receptors that activate NF-κB families of transcription factors including all Toll-like Receptors (TLRs), receptors coupled to the STAT family of transcription factors, and nuclear receptors. Tumor Necrosis Factor-alpha (TNF-α), IL-1 and others act via the NF-κB receptor family while IFN-γ and IL-4 act through STAT-1 and STAT-6 receptors respectively.

TLRs have gained traction in recent times due to the influential role played by them in activating the two arms of immunity; innate and adaptive immune responses[29]. Human cells boast of only about 25000 protein-encoding genes, making it impossible to have a different gene for all the pathogens capable of infecting humans[30]. In 1989, Charles Janeway proposed a new theory explaining that immune cells are capable of detecting specific patterns to identify foreign entities[30]. The theory further stated that the receptors bind to the structural shapes or patterns that are expressed by the invading pathogens, but not the host. The first human pattern recognizing receptors were discovered ten years after Janeway's proposal; the TLRs[30]. TLRs recognize the

highly conserved structural motifs known as pathogen-associated microbial patterns (PAMPs) expressed by microbial pathogens and danger-associated molecular patterns (DAMPs) that are endogenous molecules secreted by necrotic, dying cells[31]. Significant progress has been achieved in understanding the TLR function[32]. TLR signaling is paramount in eradicating microbial infections and promoting tissue repair. Several therapeutic agents targeting TLRs are currently undergoing clinical trials[33]. However, TLRs can act as double-edged swords either promoting or inhibiting disease progression. The therapeutic agents targeting the TLRs should accordingly antagonize the harmful effects without disrupting the host immune response. The TLR signaling must be tight and the strong polarizing stimuli used thus far for directed polarization have failed to find the right balance.

1.5 Re-education of Macrophages

Pro-inflammatory M1 activated macrophages could be re-educated towards the M2 phenotype and vice versa by manipulating the environmental cues. This process is referred to as macrophage re-programming or repolarization[34, 35]. The classical approach for macrophage re-programming has hinged upon the cytokine delivery. Cytokines are potent immune-modulatory agents capable of dictating the sway of macrophage population towards a particular phenotype. The switch from the pro- to anti-inflammatory phenotype (M1 to M2 phenotype) is achieved chiefly by loading the appropriate stimuli responsible for M2 differentiation, such as IL-4, IL-10 or IL-13[35]. Transformation from M1 to M2 state, desirable in systemic inflammatory diseases involves delivery of anti-inflammatory related cytokine miRNA or plasmid DNA. However, the mechanism of reprogramming has not been elucidated to date necessitating the need for further investigations.

1.6 Current Approaches: Nanomaterials

Nanomaterials have been a significant focus in immunotherapy and have shown initial promise in activation, regulation and resolution of immune responses *in vivo*[36]. Nanomaterials are capable of translocating to the tissues and, as foreign entities, are highly likely to encounter innate immune cells[37]. The potential of metallic NPs in activation of innate immunity as well as induction of inflammasome formation has been documented in literature[38]. Heavy metals and other metallic NPs possess the ability to activate pathways controlling inflammation through regulatory interactions with innate immune cells[39, 40, 41, 42, 43, 44]. NPs afford flexibility in terms of size, shape and surface modification enabling specific targeting, longer duration of action and reduced metabolic susceptibility. The biodistribution, cellular interactions and therapeutic effects of NPs can be influenced by their physical characteristics such as size and shape and their chemical nature[45, 46, 47]. Other studies have shown that surface charge of NPs also plays an important role in their cellular uptake; charged NPs being taken up to higher extent than neutral particles[48, 49].

The shape of NPs dictates the uptake, clearance and efficacy profiles as well as the possible interactions with macrophages. Until recently, reproducible synthesis of different shapes of NPs posed a challenge at the nano-scale level. As a result, role of shape received little attention in fabrication of NPs. Thus, shape as well as other shape-related parameters such as surface area and volume has received little attention compared to the size-dependent effects of nanomaterial. However, recent advances in the field of nanomaterials enable synthesis of wide ranging shapes of NPs with precision. Mitragotri *et al.* have recently explored the effect of shape and target geometry on the phagocytic abilities of macrophages[50]. They demonstrated that elongated NPs are engulfed by immune cells at much lower rates compared to spherical ones[50]. The differential phagocytic profiles of elongated compared to spherical nanomaterial would also affect other

parameters such as nanomaterial efficacy, duration of action and clearance profile[50]. Concurrent research has also focused on the use of different shapes of NPs to resemble viruses and thus, elicit an appropriate immune response[51]. Isotropic shapes like sphere have similar physical properties irrespective of their orientation. Anisotropic shapes like cube, rod and ellipsoids display different geometry depending on the orientation. The shape-dependent effect of nanomaterials on macrophage phagocytosis reveals the need to understand the effect of shape as a parameter while designing and fabricating nanomaterials, especially for immunotherapeutic approaches.

Nanomaterials have been exploited for immunotherapeutic approaches using multiple approaches. For example, delivery of cytokines *in vivo* presents various formulation problems. These formulation problems are similar to those encountered with any peptide or protein[52]. Oral bioavailability is low on account of degradation in the gastrointestinal (GI) tract as well as their inability to cross epithelial barriers. They also have high molecular weight, low lipophilicity and charged functional groups that prevent passive absorption. Cytokines also pose problems of systemic toxicity owing to their non-specificity and rapid metabolic clearance limiting duration of action. The cytokine delivery systems discussed in previous sections have thus relied on the nanomaterials as their preferred choice of vehicle to address one or more of the above-discussed problems and to either prime or re-educate the macrophage phenotype.

The TLRs responsible for priming of macrophages have been targeted by using NPs. TLR-4 has been identified as the signal transducer responsible for activation of innate immunity and pro-inflammatory cytokine production by Cobalt NPs[53]. Use of TLR-4 blocking antibodies or TLR4-negative cells block these effects while on the other hand potentiation of effect is observed in TLR4-overexpressing cells[53]. In THP-1 human monocytes, activation of TLR-4 leads to IL-8 release which in turn results in the recruitment of neutrophils and thus higher phagocytic

capabilities[54, 55]. Gold NPs accumulate in the lysosomes and inhibit TLR-9 receptor functionality. Receptor inhibition impedes binding of bacterial DNA fragments (CpG-ODN) altering the response to microbial pathogens[56].

NPs, apart from their ability to prime and activate macrophages, have also received attention for re-education of macrophages. Previous research suggests different NPs can differentially modulate macrophage phenotypes[57, 58, 59]. Plasmid DNA (expressing IL-4 or IL-10) encapsulated hyaluronic acid-polyethyleneimine NPs has proven mildly successful in murine J774A.1 macrophages upregulating certain M1 markers[20]. Modified alginate NPs loaded with murine cytokine IL-10 plasmid DNA have been probed as well for the treatment of rheumatoid arthritis[35]. Super paramagnetic iron-oxide NPs (SPIONs)[57], Polystyrene NPs[59] and Glycocalyx-mimicking NPs[60] have previously been shown to exhibit ability to switch the M2 to M1 polarization state. SPIONs act by modulating cellular iron concentration[9] while Glycol NPs interact with M2 surface receptor undergoing receptor-mediated uptake resulting in the phenotypic switch[60]. In summary, NPs have great potential in the fast emerging field of immunotherapies.

1.7 Shape-specific and Free Radical Modulating Cerium Oxide NPs (CNPs) for Immune Modulation

Cerium is the most abundant rare earth metal and belongs to the lanthanide series of the periodic table (atomic number = 58). As an element belonging to the transition metals it cycles between multiple oxidation states viz. +3 and +4 (Ce_2O_3 and CeO_2 respectively)[61]. Cerium oxide has been used industrially as an ultraviolet absorber, polishing agent, gas sensor and catalyst[61, 62, 63, 64]. CNPs have also been utilized as protective agents in cosmetic products. Recently, there has been a surge

in the biomedical applications of CNPs such as protection against radiation, cellular damage induced by toxicants and pathological conditions like brain or cardiac ischemia, neurologic disorders and neurodegeneration of retina[65].

CNPs are popular superoxide dismutase (SOD) and catalase mimetic nanomaterials. Some studies have reported the ability of CNPs to trigger pro-oxidative effect through induction of oxidative stress in the form of reactive oxygen species (ROS) while other studies depicted have shown anti-oxidant effects of CNPs *in vivo* and *in vitro,* due to their ability to scavenge free radical[66]. More accurately, CNPs exhibit either pro-oxidative or antioxidant properties depending upon the environmental status[67, 68]. The reason for the pro- and anti-oxidant effect stems from the cerium oxide lattice boasting of a cubic fluorite structure where both the oxide forms Ce^{3+} and Ce^{4+} coexist on the surface[69]. Charge deficiency due to presence of Ce^{3+} is compensated for by oxygen deficiency in the lattice. At the nanoscale, cerium oxide contains oxygen defects which act as hotspots for its redox catalytic activity. The concentration of oxygen defects has been shown to increase with a decrease in particle size[69]. The relative ratio of Ce^{3+} and Ce^{4+} on the surface at a given time dictates its pro- or anti-oxidant activity[69]. The two oxidation states can easily switch back and forth due to the low reduction potential (~1.52V) of the Ce^{3+}/Ce^{4+} couple. This property renders CNPs virtually regenerative free radical modulators leading to longer duration of action[70].

Other studies have explored antibacterial activity of CNPs against gram-negative bacteria like *Pseudomonas aeruginosa* and *E. coli*, and gram-positive *Bacillus subtilis*[71, 72]. The mechanism of action is believed to be based on the ROS modulation activity of CNP. CNPs are thus emerging as attractive nanomaterial for biomedical applications.

In addition to their unique regenerative free radical modulating property, CNPs can be synthesized in various shapes. Mai *et al.* used hydrothermal method to synthesize CNPs in different shapes by

controlling the molarity of sodium hydroxide (0.01- 9M) and temperature (100^0-180^0C)[73]. However, interplay between CNP shapes and their free radical modulating activity in guiding macrophage polarization has not been studied.

In summary,

1. Microenvironmental factors play a key role in dictating the predominant phenotype of macrophages. For example, inflammatory status, presence of ROS/RNS etc. can control the phenotypic changes associated with the macrophages.

2. Physical properties of NPs such as shapes mimicking various pathogens are also shown to affect their uptake by macrophages and can be exploited for guiding macrophage polarization.

3. CNPs are capable of modulating the free radical levels of ROS/RNS affecting the inflammatory status of the microenvironment.

4. CNPs can be synthesized in various shapes such as isotropic sphere, and anisotropic cubes and rods with different aspect ratios.

Thus, ability to synthesize CNPs in different shapes along with their free radical modulating activity enables us to investigate the causal relation between CNP shapes and ROS/RNS levels in the microenvironment surrounding M1/M2 macrophages and how these two factors combined together further guide macrophage polarization. In this study, we hypothesized that the shape specific CNPs can influence the macrophage phenotypes through their dual attributes: free radical modulating ability and their shapes with various aspect ratios.

2.0 MATERIALS AND METHODS

2.1 Synthesis of Shape-specific CNPs

CNPs synthesized for the purpose of subsequent experiments are denoted based on their shape as observed in Transmission Electron Microscopy (TEM), viz. Sphere, Cube, and Rod. Spherical CNPs were prepared by ultra-sonication[74] method while Cube and Rod CNPs were synthesized using hydrothermal method[73].

Sphere CNPs: Cerium nitrate hexahydrate (5g, Sigma Aldrich, USA) and methoxy polyethylene glycol (mPEG, 1g, 5000 Da, Acros Organics, USA) were dissolved in deionized water (100mL). Sodium hydroxide solution (5mg/mL in deionized water, Sigma Aldrich, USA) was added at a rate of 5mL/min under constant stirring and sonication until pH of 10 was achieved **(Figure 2A)**. The NP suspension was allowed to stand and the resulting supernatant was discarded. The CNPs were then washed with deionized water several times to remove traces of unreacted sodium hydroxide until the pH of the supernatant was neutral followed by final wash with ethanol. CNPs were then obtained by centrifugation followed by overnight drying at 100^{o}C in oven.

Cube/ Rod CNPs: Cerium nitrate hexahydrate (0.868g) was dissolved in deionized water (5mL) and added in a drop-wise manner (at rate of 1mL/min, **Figure 2C**) to sodium hydroxide solution (35 mL, 6M for Cube and 9M for Rod) under constant stirring for 30 minutes at room temperature. The solution was then sealed in a hydrothermal reactor and allowed to react at 100 °C (Rod) or 180 °C (Cube) for 24 h **(Figure 2B)**. Subsequently, CNPs were washed with deionized water and ethanol several times until the pH of the supernatant became neutral. CNPs were obtained by centrifugation followed by overnight drying at 60°C in oven.

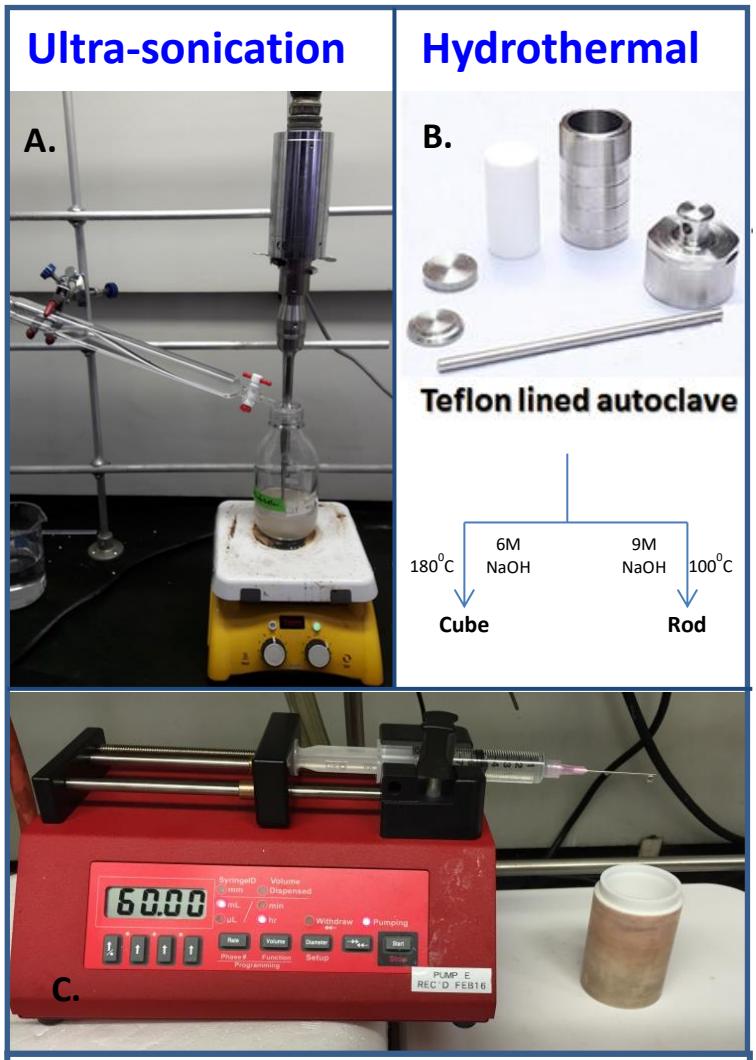

Figure 2: Instrumentation and set -up for CNP synthesis

A) Drop-wise addition of sodium hydroxide solution in ultra-sonication method for synthesis of Sphere CNPs.
B) Differences in reagent concentration and reaction temperatures for synthesis of Cube and Rod CNPs as per hydrothermal method.
C) Drop-wise addition of sodium hydroxide solution in hydrothermal method for synthesis of Cube and Rod CNPs.

2.2 Physicochemical Characterization of CNPs

2.2.1 Transmission electron microscope (TEM) Imaging:

TEM was used to determine the size and shape of synthesized CNPs in dry state. Low concentration dispersions of CNPs in acetic acid (2% v/v) were deposited on copper grids and images were acquired without any staining using electron microscope (JEOL 1011, Joel, Tokyo, Japan) operated at an accelerating voltage of 80 kV.

2.2.2 Size, size distribution, and zeta potential:

Size, size distribution (hydrodynamic diameter) and zeta potential were measured by dynamic light scattering (DLS) (Zetasizer 3000, Malvern, USA). A stock solution of CNPs (1mg/mL) in HEPES buffer was prepared (pH 4.0, 10mM, G.E. Healthcare, USA) and subjected to the probe sonication (10% Amplitude, On/Off Pulse- 15:10 seconds, Sonic Dismembrator Model 500, Fisher Scientific, USA) for 20 minutes for obtaining a uniform dispersion. The dispersion was subsequently diluted to 25μg/mL in THP-1 culture media (RPMI 1640 + 10% FBS + 1% Penicillin-Streptomycin).

2.3 THP-1 Cell Culture

THP-1 human monocyte derived cell line is an established model to study macrophage differentiation. THP-1 cell line was obtained from Dr. Vera Donnenberg (Department of Cardiothoracic Surgery, UPMC, Pittsburgh). All the cell culture supplies and media were obtained from Corning and Mediatech, respectively unless specified. The cell line were grown in suspension in either T-25 or T-75 culture flasks in media containing RPMI 1640 (Roswell Park Memorial Institute media) supplemented with 10% FBS (Hyclone, Utah, USA) and 1% Penicillin-

Streptomycin. The average doubling time for THP-1 was about 20-30 h. Culture was maintained at cell densities ranging between 2- 9 x 10^5 cells/mL at 37° C, under 5% CO_2.

2.4 Optimization of THP-1 Differentiation to Macrophages

The first goal of the study was to develop protocol to reproducibly differentiate human THP-1 monocytes into naïve (M0), classically activated (M1) and alternately activated (M2) macrophages. The differentiation of THP-1 monocytes into macrophages is primarily conducted using phorbol 12-myristate 13-acetate (PMA). PMA is a diester of phorbol and a potent tumor promoter employed in research to activate the signal transduction enzyme protein kinase C (PKC)[75]. PMA treatment results in cell adherence and terminates cell proliferation producing naïve M0 macrophages. The naïve M0 macrophages were further provided specific stimuli to differentiate them towards M1 and M2 macrophages. For M1 differentiation, M0 macrophages were treated with combination of lipopolysaccharide (LPS) and interferon-gamma (IFN- γ) (henceforth treatment is abbreviated as LPS + IFN-γ) while for M2 differentiation, M0 macrophages were further treated with combination of interleukin 4 and 13 (IL-4 + IL-13).

We subsequently calibrated the concentrations and duration of above treatments to reproduce the three phenotypes consistently. This is important since it is known that high concentrations of PMA by itself can upregulate expression of M1 genes, overwhelming the effects induced by other treatments[76]. We tested three different differentiation protocols independently (n=4 from two independent experiments) using mRNA expressions of markers specific for M1 (*iNOS, IL-12, TNF-α*) and M2 (*Arginase, IL-10, TGF-β*) phenotypes by real time quantitative polymerase chain reaction (RT-qPCR). The protocols are as follows:

Protocol 1:

Seeding Density: 0.5 x 10^6 cells/well (6-well plate)

PMA Treatment: 100ng/well for 72 h (M0 differentiation)

Resting Phase: Remove PMA and incubate in fresh RPMI media for 24 h

Final Treatment: LPS + IFN-γ; 20ng/mL for 48 h (for M1 differentiation) OR

IL-4 + IL-13; 20ng/mL for 48 h (for M2 differentiation)

Protocol 2:

Seeding Density: 1 x 10^6 cells/well (6-well plate)

PMA Treatment: 20ng/well for 24 h (M0 differentiation)

Resting Phase: Remove PMA and incubate in fresh RPMI media for 24 h

Final Treatment: LPS + IFN-γ; 10ng/mL for 24 h (for M1 differentiation) OR

IL-4 + IL-13; 10ng/mL for 24 h (for M2 differentiation)

Protocol 3:

Seeding Density: 1.5 x 10^6 cells/well (6-well plate)

PMA Treatment: 35ng/well for 24 h (M0 differentiation)

Resting Phase: No resting phase

Final Treatment: LPS + IFN-γ; 10ng/mL for 18 h (for M1 differentiation) OR

IL-4 + IL-13; 10ng/mL for 18 h (for M2 differentiation)

The efficiency of differentiation of THP-1 cells to M0, M1 and M2 by the three different protocols was compared by calculating M1/M2 ratio for each marker as demonstrated below for *iNOS*.

$$\frac{\mathrm{M1_{iNOS}}}{\mathrm{M2_{iNOS}}} = \frac{iNOS\ expression\ \ post\ LPS + IFN - \gamma\ treatment}{iNOS\ expression\ post\ IL-4 + IL-13\ treatment}$$

2.5 RNA Isolation and RT-qPCR Analysis

Gene expression profiles of each macrophage phenotype (M0, M1, M2) were assessed by real time quantitative polymerase chain reaction (RT-qPCR). Expression of three M1 markers (*iNOS, IL-12 and TNF-α*) and three M2 markers (*Arginase, IL-10 and TGF-β*) were measured while β-Actin was used as a loading control. These markers were selected from the literature[77, 78]. Naïve M0 macrophages were considered as the experimental control. RNA was isolated using GeneJET RNA purification kit (Thermo Scientific, Lithuania, EU) according to manufacturer's protocol. Briefly, the cells were differentiated using Protocol #2 or #3. After treatment the scraped cell pellet was suspended in lysis buffer (supplemented with 14.3M β-Mercaptoethanol, 20μL/mL), followed by short vortexing, ethanol addition and passage through the GeneJET purification column. After multiple washings with the buffers provided with the kit and subsequent centrifugations at 12,000 RPM, the total RNA adsorbed onto the column was finally eluted using nuclease free water. RNA concentration in the eluted water was measured using spectrophotometer (Nanodrop 2000, Thermo Scientific, USA) and the RNA quality was assessed by measuring the absorbance ratio at 260/280 nm. The mRNA expression of the seven markers was measured by RT-qPCR using iTaq Universal SYBR Green RT-PCR kit (BioRad Laboratories Inc., USA).

Table 1: Primer sequences of M1 and M2 markers

mRNA Markers	Forward Primer	Reverse Primer
B-Actin	5'- ACCTTCTACAATGAGCTGCG-3'	5'-CCTGGATAGCAACGTACATGG-3'
iNOS	5'-GTTCTCAGGCCAACAATACAAGA-3'	5'-GTGGACGGGTCGATGTCAC-3'
IL-12	5'-TGGTTTGCCATCGTTTTGCTG-3'	5'-ACAGGTGAGGTTCACTGTTTCT-3'
TNF-α	5'-AGACGCCACATCCCCTGACAA-3'	5'-AGACGGCGATGCGGCTGATG-3'
Arginase	5'-TTCTCAAAAGGACAGCCTCG-3'	5'-AGCTCTTCATTGGCTTTCCC-3
IL-10	5'-CAGAGCCACATGCTCCTAGA-3'	5'-TGTCCAGCTGGTCCTTTGTT-3'
TGF-β	5'-TGGAGCAACATGTGGAACTC-3'	5'-CAGCAGCCGGTTACCAAG-3'

Each reaction mixture (10μL) contained 5 ng mRNA, 2x SYBR Green master mix (5μL), iScript Reverse transcriptase (0.125μL) and respective primers (0.2μM) in duplicates. The amplification protocol consisted of 40 cycles of denaturation for 15s at 95^{o}C, annealing for 30s at 55^{o}C and extension for 30s at 72^{o}C (7500 Fast Real-Time PCR System, Applied Biosystems, California, USA). The mRNA expression was calculated using 2-ΔΔCt method[79] and depicted as the mean ± SEM as fold change compared to the controls (n=4 from two independent experiments).

2.6 Dose-dependent Effect of CNPs on Viability of Pre-differentiated Macrophages

The dose-dependent cytotoxicity of CNPs was determined by alamarBlue® assay (Thermo Scientific, USA) according to the manufacturer's protocol. Resazurin, the active ingredient of alamarBlue® reagent, is a non-toxic, cell permeable compound that is blue in color and virtually non-fluorescent. Upon entering cells, resazurin is reduced to resorufin, a compound that is red in color and highly fluorescent. Viable cells continuously convert resazurin to resorufin, increasing the overall fluorescence and color of the media surrounding cells.

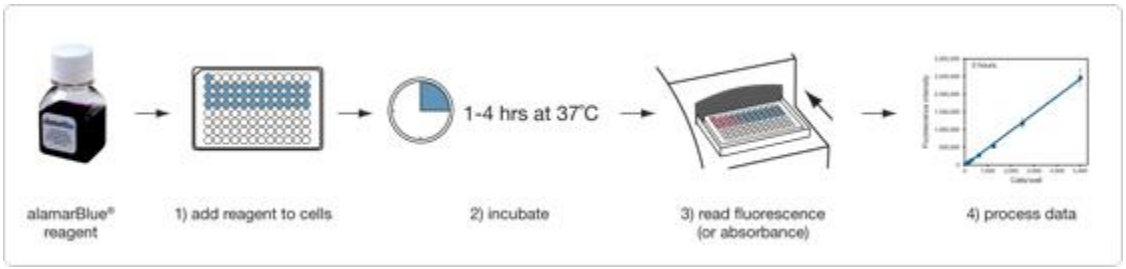

THP-1 cells (50,000/well) were seeded in a 96-well plate and Protocol #3 was followed for subsequent differentiation. The pre-differentiated (M0, M1, M2) macrophages were then treated with varying concentrations of CNPs (0, 1, 5, 10, 25, 50, 100, and 250µg/mL in THP-1 culture media) to obtain the concentration curve for each CNP shape (Sphere, Cube, Rod). After 24 h of CNP treatment the cells were incubated with alamarBlue® solution (100µL/well, 10%v/v in THP-1 culture media) for 3 h. Subsequently the fluorescence intensity was measured at excitation/emission wavelength of 530/590 nm using a microplate reader (Synergy HT, BioTek instruments, USA). Each of the pre-differentiated macrophage phenotype (M0, M1, M2) treated with the culture media (0µg/mL CNPs) served as its own negative control (considered as 100% viable) (n=6 from two independent experiments). The percentage viability for each CNP concentration was then calculated using the formula mentioned below.

$$\% \text{ Viability } = \frac{\text{RFU}_{\text{CNP}}}{\text{RFU}_{\text{negative}}} x\, 100\%$$

2.7 Dose-dependent Effects of CNPs on the Intracellular Reactive Oxygen Species (ROS)

The intracellular ROS levels in pre-differentiated (M0, M1, M2) macrophages were measured using 2,7-Dichlorodihydrofluorescein diacetate (DCFH-DA) assay (Cayman chemical, USA). DCFH-DA is a fluorescent dye that measures hydroxyl, peroxyl and other ROS activity within the cell. After diffusion in to the cell, DCFH-DA is de-acetylated by cellular esterases to a non-fluorescent compound, which is later oxidized by ROS into 2', 7' –dichlorofluorescein (DCF). DCF is a highly fluorescent compound, which can be measured by fluorescence spectroscopy.

The THP-1 cells were pre-differentiated to the respective phenotype using Protocol #3 followed by 30 minutes incubation at 37^{o}C in DCFH-DA (20µM, 100µL) in Hank's Balanced Salt Solution (HBSS). DCFH-DA solution was removed at the end of the incubation period and washed with HBSS. Subsequently the cells were treated with CNPs (0, 5, 25, 100µg/mL) for different duration of time (6, 12, 24 h). For the purpose of comparison, the cells were seeded at uniform density and the concentration of CNPs were maintained such that no severe cell death occurred, ensuring that fluorescence intensity was not influenced by these parameters. Fluorescence intensity of DCF was measured at excitation/emission wavelength of 485/528 nm using a microplate reader (Synergy HT, BioTek instruments, USA). Cells receiving only fresh THP-1 culture media (0µg/mL CNPs) were served as negative control (baseline ROS levels) in these experiments. Each pre-differentiated phenotype had its own negative control (considered as 100% ROS level) (n=6 from two independent experiments). The percentage ROS for each condition was calculated using the formula mentioned below.

$$\% \text{ ROS } = \frac{\text{RFU}_{\text{CNP}}}{\text{RFU}_{\text{negative}}} x\, 100\%$$

2.8 Dose-dependent Effects of CNPs on the Extracellular Reactive Nitrogen Species (RNS)

The extracellular RNS levels in pre-differentiated (M0, M1, M2) macrophages were measured using Griess reagent (Promega, USA) following the manufacturer's guidelines. The Griess reagent assay is based on the chemical reaction, which uses sulfanilamide and N-1-napthylethylenediamine dihydrochloride (NED) under acidic (phosphoric acid) conditions. This system detects nitrite (NO^{2-}) concentration secreted extracellularly in the cell culture medium. The standard curve was constructed using known concentrations of nitrite solution (in culture media) provided by the manufacturer.

The cells were pre-differentiated using Protocol #3, and were treated with CNPs (0, 5, 25, 100µg/mL) for different duration of time (6, 12, 24 h) as described under **section 2.7**. After the treatment, the supernatant culture media was collected from each well for measuring RNS levels. Nitrate reductase co-factor and enzyme (10µL each, Cayman Chemicals, USA) were added sequentially to the collected supernatant culture media (80µL). The plate was then placed in a Thermomixer R (Eppendorf, Germany) at 37°C, 300 rpm for 2 h. Subsequently Griess reagent sulfanilamide solution and NED solution were added (50µL each) and incubated for 10 minutes to allow color development. The absorbance was measured at wavelength of 540/550nm using a microplate reader (Synergy HT, BioTek instruments, USA). The RNS levels (µM) were obtained by interpolating the standard curve. Supernatants collected from cells receiving only THP-1 culture media without any CNP treatment were considered as negative control (baseline RNS levels) for

these experiments (n=6 from two independent experiments). Each pre-differentiated phenotype had its own negative control (considered as 100% RNS level) and the percentage RNS for each condition was calculated using the formula mentioned below.

$$\% \text{ RNS } = \frac{\text{RFU}_{\text{CNP}}}{\text{RFU}_{\text{negative}}} x\ 100\%$$

2.9 Dose-dependent Effects of CNPs on Macrophage Polarization

Gene expression profiles of each macrophage phenotype (M0, M1, M2) following CNP treatment was assessed by RT-qPCR to determine the priming or re-programming effects. The cells were pre-differentiated using Protocol #3 and were treated with CNPs (0, 5, 25, 100μg/mL) for 12 h. After the treatment, the scraped cell pellet was subjected to RT-qPCR following the protocol outlined in **section 2.5**. Each of the pre-differentiated macrophage phenotypes (M0, M1, M2) treated with the culture media (0μg/mL) served as their respective negative control (n=4 from two independent experiments). An M1/M2 ratio was calculated by pairing up one marker each of M1 and M2 respectively. The pairing was performed on the basis of similarities between the two markers. Thus, *iNOS* was paired with *Arginase-1, IL-12* with *IL-10* and *TNF-α* with *TGF-β*. For treatment with LPS+IFN-γ, where the expected predominant phenotype is M1, M1 marker expression is expected to be higher than that of the M2 marker and hence, an M1/M2 ratio was plotted (represented as positive M1/M2 ratio plotted on positive y-axis). On the other hand, for treatment with IL-4+IL-13, where the expected predominant phenotype is M2, the expression of M2 marker is expected to be higher than that of M1 marker, and hence, an M2/M1 ratio was calculated in a similar manner (represented as negative M1/M2 ratio plotted on negative y-axis).

2.10 Effects of Inhibition of ROS with Co-administration of Anti-oxidant (NAC) and CNPs on ROS/RNS Levels and Macrophage Polarization

In order to delineate role of ROS generated by CNPs to guide macrophage polarization, different macrophage phenotypes were treated with a widely used anti-oxidant, N-acetyl cysteine (NAC)[80] prior to CNP treatment. Briefly, the cells were pre-differentiated (Protocol #3) to M1 or M2 followed by treatment with NAC (1μM) for 3 h. These cells were then treated with Rod or Cube CNPs (100μg/mL, 12 h) without removing the NAC containing media. CNP dose of 100μg/mL was selected based on the results of previous experiment (**Section 2.9**) studying effects of CNPs on macrophage polarization (see **Results and Discussion**). Untreated M1 and M2 cells were considered as baseline control while NAC treated cells without CNP treatment were designated as negative control (n=4 from two independent experiments). At the end of the experiments, ROS/RNS levels as well as mRNA expression of M1 and M2 markers were measured. Data represented as mean ± SD or mean ± SEM, respectively.

2.11 Effects of Inhibition of RNS with Co-administration of NOS Inhibitor (L-NAME) and CNPs on ROS/RNS Levels and Macrophage Polarization

We further asked if the asked if the ability of CNPs to modulate macrophage phenotype is linked to its RNS modulating effects by using a pan-nitric oxide synthase (NOS) inhibitor. L-NAME (L-N^G-Nitroarginine methyl ester) is a widely used inhibitor of NOS isoforms and acts by inhibiting cGMP formation[81]. Briefly, the cells were pre-differentiated (Protocol #3) to M1 or M2 followed by treatment with L-NAME (1μM) for 3 h. These cells were then treated with Rod or Cube CNPs (100μg/mL, 12 h) without removing the L-NAME containing media. Untreated M1 and M2 cells

were considered as baseline control while L-NAME treated cells without CNP treatment were designated as negative control (n=4 from two independent experiments). At the end of the experiments, ROS/RNS levels as well as mRNA expression of M1 and M2 markers were measured. Data represented as mean ± SD or mean ± SEM, respectively.

2.12 Statistical Analysis

Results are presented as either mean ± standard error of the mean (SEM) or mean ± standard deviation (SD) as specified in each figure legend. Results are compiled from at least two individual experiments each with two or more replicates. Multiple comparisons were analyzed for significance using one-way analysis of variance (ANOVA) or two-way ANOVA followed by Tukey's post-hoc analysis as appropriate, with $p = 0.05$ as the significance cutoff.

3.0 RESULTS AND DISCUSSION

3.1 Physicochemical Characterization of CNPs

We have previously demonstrated our ability to reproducibly synthesize four different shapes of CNPs[82]. The established protocols as mentioned in **Section 2.1** were followed for the synthesis. Measurement of the true size and aspect ratio (height: width ratio) of the inorganic core of CNPs was facilitated by TEM imaging **(Figure 3A and 3B)**. All shapes of CNPs displayed sizes in the sub-100nm range. TEM measures the size of CNPs in their original state. The macrophages, however, will encounter CNPs in hydrated state necessitating measurement of hydrodynamic size.

Previous data from the lab has suggested that CNPs disperse primarily in HEPES buffer (10mM, pH 4.0) after probe sonication (for 20 minutes)[82]. Subsequent dilution in culture media containing serum yielded stable CNP suspension displaying no signs of excessive agglomeration or sedimentation.

Since all the subsequent cell experiments were carried out in THP-1 culture media, RPMI 1640 media containing serum was chosen as the preferred solvent for CNP dispersion and further characterization. The table 2 **(Figure 3C)** shows the results for size distribution and zeta potential of different shapes of CNPs. The size distribution in THP-1 culture media was measured with

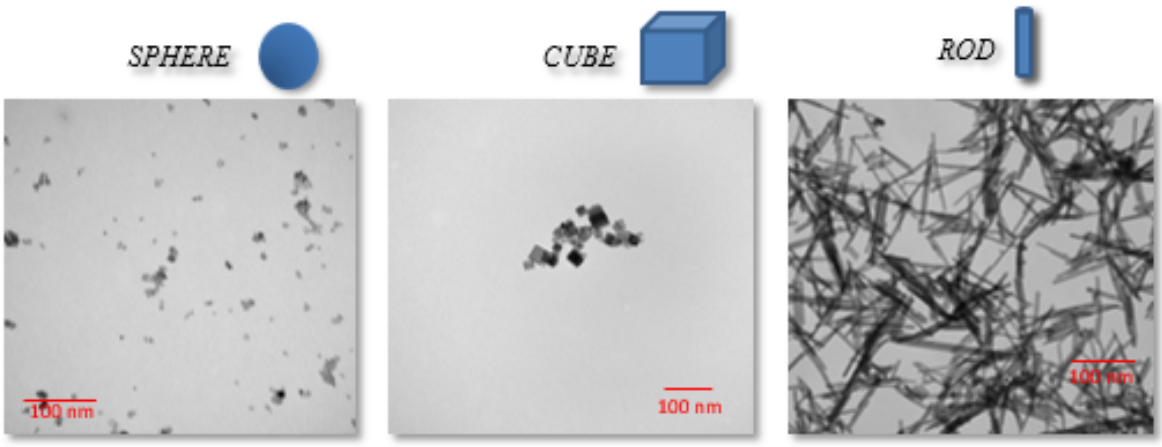

Table 1:

	Sphere	Cube	Rod
Aspect ratio	1:1	1:1	21:1

Table 2:

	Size ± SD (d.nm)	PDI ± SD	Zeta ± SD (mV)
Sphere	169 ± 2.350	0.243 ± 0.011	-12.8 ± 0.868
Cube	166.2 ± 1.159	0.236 ± 0.002	-12.3 ± 0.624
Rod	238.9 ± 4.33	0.223 ± 0.021	-12.0 ± 0.346

Figure 3: Characterization of Cerium Oxide Nanoparticle (CNP) Characterization

A) TEM images of Sphere, Cube and Rod CNPs were acquired without staining. Scale bar = 100nm.

B) Table 1 shows the different aspect ratios (height: width) of Sphere, Cube and Rod CNPs.

C) Table 2 summarizes the particle size and zeta analysis. Stock CNP dispersions (1mg/mL in HEPES buffer) were diluted in THP-I culture media prior to measurements.

DLS and was consistent with our published data[82]. Sphere and Cube CNPs were found to be in the sub-200 nm size range while Rod CNPs measure approximately 240nm in diameter. The DLS method provides values that denote apparent size (hydrodynamic diameter) of the NPs. Any macromolecule in a solution encounters a thin electric dipole layer of solvent, which adheres to its surface. The apparent size thus provides information about the inorganic core of CNPs as well as the adherent solvent layer.

The magnitude of the charge as measured by zeta potential is indicative of the potential stability of the colloidal system. All CNPs irrespective of their shapes showed negative zeta potential when dispersed in culture media. The negative charge can be attributed to the culture media and serum. CNPs diluted in water showed positive zeta potential (unpublished data). The negative charge on CNPs in culture media suggests that the CNPs tend to repel each other in the suspension and thus, will have lower tendency to agglomerate. The CNP dispersion is prepared fresh for each experiment and administered to the cells within few hours of dispersion.

3.2 Optimization of THP-1 Differentiation to Macrophages Phenotypes

THP-1 is a spontaneously immortalized monocyte-like cell line, derived from the peripheral blood of a childhood case of acute monocytic leukemia (M5 subtype)[83]. The THP-1 cell line is often used as a substitute *in vitro* model for human peripheral blood monocytes (primary) *ex vivo*. The first optimization step in the experiment involved differentiation of THP-1 human monocytes into naïve macrophages (M0), classically activated (M1) and alternately activated (M2) macrophages. Different stimuli have been used in many different labs for obtaining the differentiated macrophage phenotypes. The most commonly used stimulus to differentiate the human monocytes to naïve

macrophages (M0) is PMA. Also known as Tumor Promoting Agent (TPA), PMA is used to differentiate monocytes to macrophages, boost cytokine production as well as for T-cell activation[76]. The mechanism of action of PMA is attributed to its similarity with diacylglycerol, an endogenous Protein Kinase C (PKC) activator[76]. The use of PMA results in activation of inflammasome. As mentioned previously, the THP-1 cell line is an established model to study inflammasomes. Inflammasomes are responsible for activation of inflammatory processes[84]. PMA also promotes the formation of inflammatory cytokines such as Interleukin-1β (IL-1 β) and Interleukin-18 (IL-18)[85].

The secondary stimulus to differentiate naïve macrophages towards classically activated M1-like macrophages involves use of LPS and IFN-γ. LPS is a major structural component of bacteria present in the outer membrane of the cell wall which mimics gram negative infection both *in vivo* and *in vitro*[86]. LPS treatment thus elicits a strong immune response in the cells. LPS alone is also known to polarize macrophages into M1 phenotype, however the concomitant use of IFN-γ results in optimal M1 polarization with distinct upregulation of M1 markers. IFN-γ, a Th1 cytokine is known to activate macrophages, which in turn produces a number of pro-inflammatory cytokines[86]. Although PMA alone is capable of activating the inflammasome evident by the presence of pro-inflammatory cytokines like IL-1β, LPS is required for priming the macrophages which promotes the accumulation of cytosolic stores of pro-IL-1β, a precursor of the cytokine[85]. The IL-1β produced subsequently induces its own synthesis sustaining the pro-inflammatory conditions for longer duration[86]. The sequential treatment of PMA followed by LPS and IFN-γ thus provides a robust combination to obtain the classically activated M1 macrophages.

M2 macrophage differentiation can be induced by different stimuli; IL-4 and/or IL-13, immune complexes and toll-like receptor, IL-1 receptor ligands or IL-10[87]. The cytokines IL-4 and IL-13

share a strong homology and overlap functionally[88]. It has been demonstrated that IL-4 and IL-13 are capable of stimulating IL-10 production, a cytokine, which acts as a negative feedback to release pro-inflammatory cytokines like TNF-α and IL-6. IL-4 and IL-13 are also responsible for secretion of anti-inflammatory cytokines such as CCL18 and CCL22, expression of mannose receptors like CD206 and scavenger receptor CD163[78, 88]. IL-4 is more potent *in vitro* than IL-13; however their combined treatment is often used for optimal differentiation towards M2-like phenotype[88]. Hence, we used the combination of IL-4 and IL-13 treatments as the secondary stimulus following PMA treatment for differentiation to M2 phenotypes.

After selection of the appropriate stimuli to be used for polarization of macrophages, the next step of optimization involved determination of the concentration and duration of treatment for each of the steps in the differentiation. All of the above reagents are potent entities and thus the concentration and duration are important parameters to ensure efficient differentiation towards a predominantly desired phenotype without causing toxicity to the cells and hampering the reproducibility. Three different protocols **(Section 2.4)** and tested using mRNA expression levels of M1 and M2 markers as a read-out to determine the predominant phenotype and thus, compare the differentiation efficiency of the protocol. The cells which received just the PMA treatment (M0 macrophages) were used as experimental controls (baseline macrophage phenotype) and as normalization factor to calculate the fold change in mRNA expression.

Protocol #1 involved use of higher concentration of PMA, which resulted in cell lysis. The cell lysis was evident in the microscopic images taken after PMA treatment for 72 h (not shown). As a result of the apparent cell lysis, mRNA expression for Protocol #1 was not tested.

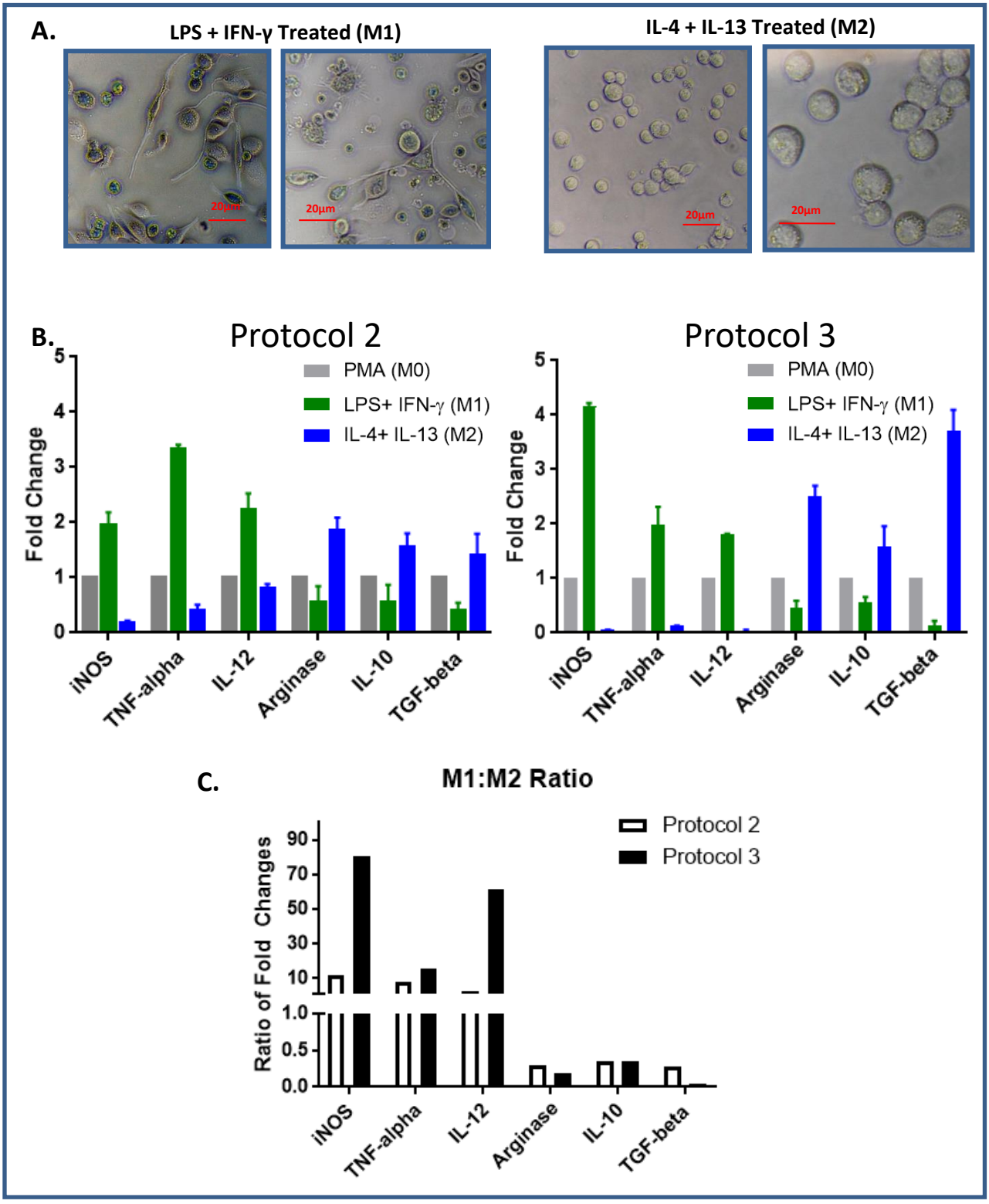
A.
LPS + IFN-γ Treated (M1)
IL-4 + IL-13 Treated (M2)
20µm
B.
Protocol 2
Protocol 3
PMA (M0)
LPS+ IFN-γ (M1)
IL-4+ IL-13 (M2)
Fold Change
iNOS
TNF-alpha
IL-12
Arginase
IL-10
TGF-beta
C.
M1:M2 Ratio
Protocol 2
Protocol 3
Ratio of Fold Changes

Figure 4: Optimization of Macrophage Differentiation Protocol

A) Representative microscopic images of M1 and M2 macrophages. Scale bar = 20μm.

B) THP-I human monocytes were differentiated to M0 (PMA treated), M1 (PMA+LPS+IFN-γ) and M2 (PMA+IL-4+IL-13) phenotypes using Protocol 2 or Protocol 3 (n=4, two independent experiments). At the end of each protocol, mRNA expression of three M1 *(iNOS, IL-12, TNF-α)* and M2 *(Arginase, IL-10, TGF-β)* markers were measured via RT-qPCR and plotted as fold change using M0 macrophages as baseline control for this experiment.

C) The effectiveness of the protocol was compared by taking a ratio for each marker in LPS+IFN-γ-treated and IL-4+IL-13-treated cells and plotted as a fold change. Protocol 3 was more effective in polarizing the macrophages than Protocol 2 as shown by much higher fold changes in M1 markers while keeping M2 marker expression to minimal levels.

The subsequent protocols were then designed to minimize exposure to PMA by reducing the duration as well as concentration of treatment. Both protocol #2 and #3 did not show any signs of cell lysis as observed in protocol #1. The LPS+IFN-γ-treated cells displayed 'spread' morphology characteristic of M1 macrophages while IL-4+IL-13-treated M2 macrophages displayed 'rounded' morphology (**Figure 4A**).

To determine which protocol was more efficient in guiding macrophage differentiation to a desired M1 or M2 phenotype, we measured mRNA expression of six markers, three each for M1 and M2 phenotypes for each cell sample. For the M0 cells treated with LPS+IFN-γ to facilitate differentiation to M1 phenotype, M1 markers *(iNOS, IL-12, TNF-α)* are expected to be significantly upregulated with low levels of M2 markers in the same cell population (green bars, **Figure 4B**). On the other hand, the cells receiving IL-4+IL-13 treatment to guide differentiation to M2 phenotype are expected to have M2 markers *(Arginase, IL-10, TGF-β)* significantly upregulated compared to the corresponding M1 markers in the same cell population (blue bars, **Figure 4B**).

Each of the protocol (#2 and #3) was capable of producing the desired outcome **(Figure 4B)**. LPS+IFN-γ treatment resulted in upregulation of all the M1 markers, with low levels of M2 marker expression (green bars, **Figure 4B)**. In contrast, the cells receiving IL-4+IL-13 treatment showed

increased expression of M2 markers with reduced expression of M1 markers (blue bars, **Figure 4B)**. Protocol #2 displayed highest expression of *TNF-α* and *Arginase* amongst M1 and M2 markers, respectively; while Protocol #3 displayed highest expressions of *iNOS* and *TGF-β* amongst M1 and M2 markers, respectively. As all the markers evaluated showed similar trends, it was concluded that both the protocols were able to polarize macrophages to the desired M1 or M2 macrophage phenotypes.

The difference between the two protocols mainly lies in the presence or absence of the resting phase and duration of treatments of either LPS+IFN-γ or IL-4+IL-13. PMA has been shown to exert a pro-M1 like bias upon the cells[89]. As mentioned previously, PMA can activate the inflammasome pathway and trigger release of pro-inflammatory cytokines. The presence of a resting phase involves addition of THP-1 media alone devoid of any stimulus to wane off the PMA effects. On the other hand, absence of any resting phase results in continuous stimulation of macrophages for shorter duration. To determine the cumulative effect of each of the protocols followed, the ratio of the fold change for each marker was calculated for M1 and M2 macrophages as outlined below by taking an example of M1 marker, *iNOS:*

$$\frac{\mathrm{M1_{iNOS}}}{\mathrm{M2_{iNOS}}} = \frac{iNOS\ expression\ \ post\ LPS + IFN - \gamma\ treatment}{iNOS\ expression\ post\ IL - 4 + IL - 13\ treatment}$$

The protocol in which *iNOS* (and other M1 markers) were highly expressed upon LPS+IFN-γ treatment and minimally expressed following IL-4+IL-13 treatment was considered optimal for differentiation towards M1 phenotype. On the other hand, higher expression of *Arginase* upon IL-4+IL-13 treatment with low expression following LPS+IFN-γ was desired for differentiation towards M2 phenotype. This shows specificity of LPS+IFN-γ or IL-4+IL-13 treatment to drive the desired phenotype (M1 or M2, respectively) keeping the other phenotype population to minimum.

Calculation of such a ratio for each marker in Protocol #2 and #3 yielded **Figure 4C.** A higher ratio for M1 markers (*iNOS, IL-12, TNF-α)* and a lower ratio for M2 markers *(Arginase, IL-10, TGF-β)* were the preferred criteria for selecting the optimum protocol. Protocol #3 performed significantly better for all the markers except for IL-10 marker where it showed differentiation efficacy identical to the Protocol #2. With these comparatively larger differences in M1 and M2 marker expression in protocol #3 vs. protocol #2, protocol #3 was chosen for all further studies.

3.3 Cytocompatibility of CNPs in All Three Macrophage Phenotypes

We next set out to determine the dose effect of different shaped CNPs on the viability of different macrophage phenotypes including naïve M0, M1 and M2. Seven different concentrations were tested for all three shapes of CNPs in the pre-differentiated (M0, M1, M2) macrophages. The percentage of viability was calculated as mentioned in **Section 2.6** and plotted on a logarithmic concentration scale for each phenotype comparing the three different shapes **(Figure 5)**. The CNPs were well tolerated by M2 pre-differentiated macrophages followed by M0 and M1 phenotypes respectively.

The three different shapes of CNPs did not exhibit significant differences in viability at any concentration in a particular phenotype. The cytocompatibility studies revealed that different shapes of CNPs were well tolerated by M0, M1 and M2 macrophages up to concentrations of 100μg/mL (>70-80% viability). Hence CNP dose was restricted to 100μg/mL concentration for all further studies.

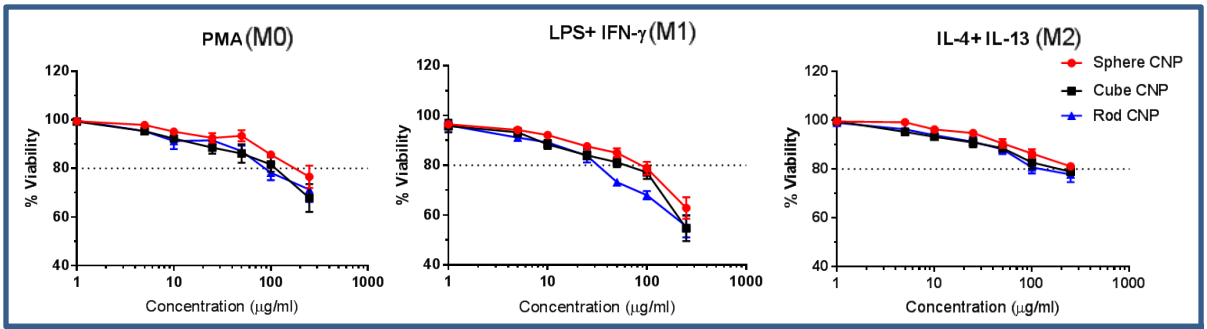

Figure 5: Cytocompatibility of CNPs in all three macrophage phenotypes

The dose-dependent cytotoxicity of CNPs was determined by alamarBlue® assay. Each pre-differentiated phenotype was subjected to different concentrations (1, 5, 10, 25, 50, 100 and 250μg/mL) of CNPs and the fluorescence read-outs were plotted as %Viability for each shape (n=6, two independent experiments). Each pre-differentiated phenotype acted as its own negative control (considered as 100% viable). CNP concentrations up to 100μg/mL were well tolerated in all three phenotypes.

3.4 Priming of Macrophages

As discussed previously (**Section 1.4**), priming of macrophages plays a key role in recruiting monocytes from the bloodstream and dictating their phenotype. Presence or absence of the immune cells in their desired phenotype often determines the disease outcome towards the progression or resolution of the disease/infection, respectively. Being the first responders, it is important that the macrophages get the right 'message' across in order to recruit other members of the immune family. Macrophages communicate and thus inform the immune system via a system of chemical messengers such as cytokines. Various disease conditions including cancers favorably alter the priming signals to suit their needs. Presence of tumor supportive Tumor-associated Macrophages (TAMs) are a good example of misguided priming of macrophages. TAMs are essentially M2-like macrophages, which promote processes such as immunosuppression, angiogenesis, invasion and metastasis[3, 90, 91, 92, 93]. Although cytokines have been widely studied for the purpose of re-

education, the initial priming and activation has received little attention so far. Some studies showed that the NPs loaded with cytokines can prime the macrophages towards a desired phenotype by acting as a stimulus in the microenvironment[57, 58, 94]. Physicochemical properties of these NPs, such as chemical composition[94], size[20] and surface coatings[95] determined the extent of priming. Graphene oxide NPs have also displayed the ability to induce inflammation in animal models by priming M0 macrophages towards M1 polarization state[96]. Hence, we first investigated effect of shape-specific CNPs on ROS/RNS levels as well as priming of naïve M0 macrophages.

To evaluate the free radical modulating activity in naïve macrophages (PMA treated M0 macrophages), the cells were treated with different CNP concentrations (5, 25, and 100μg/mL) for 12 h. **Figure 6A** shows effect of the three shapes of CNPs on the extent of free radical (ROS/RNS) levels. Untreated naïve macrophages (0μg/mL) served as a negative control. Sphere and Cube CNPs displayed similar trends across all concentrations for ROS as well as RNS levels. At higher concentrations (25, 100μg/mL), Rod CNPs showed significantly higher free radical levels compared to either Sphere or Cube CNPs and displayed dose-dependent effects.

We then measured gene expression of selected M1 and M2 markers (5, 25 and 100μg/mL). To demonstrate the predominant macrophage phenotype (M1 vs. M2) after CNP treatments, we calculated the ratio of paired M1 and M2 marker expression levels (either M1/M2 for M1 dominant phenotype or M2/M1 for M2 dominant phenotype) as described in **Section 2.9**. To accomplish this, we paired M1 and M2 markers to calculate their ratios as follows: *iNOS* with *Arginase*; *IL-12* with *IL-10*; and *TNF-α* with *TGF-β*. *iNOS* and *Arginase* were paired together as they form two distinct and opposite branches of the arginine metabolism, *IL-12* and *IL-10* designate interleukins acting as pro- and anti-inflammatory cytokines, respectively while *TNF-α* and *TGF-β* display antagonistic corollary in tissue repair through type I collagen production [97, 98, 99].

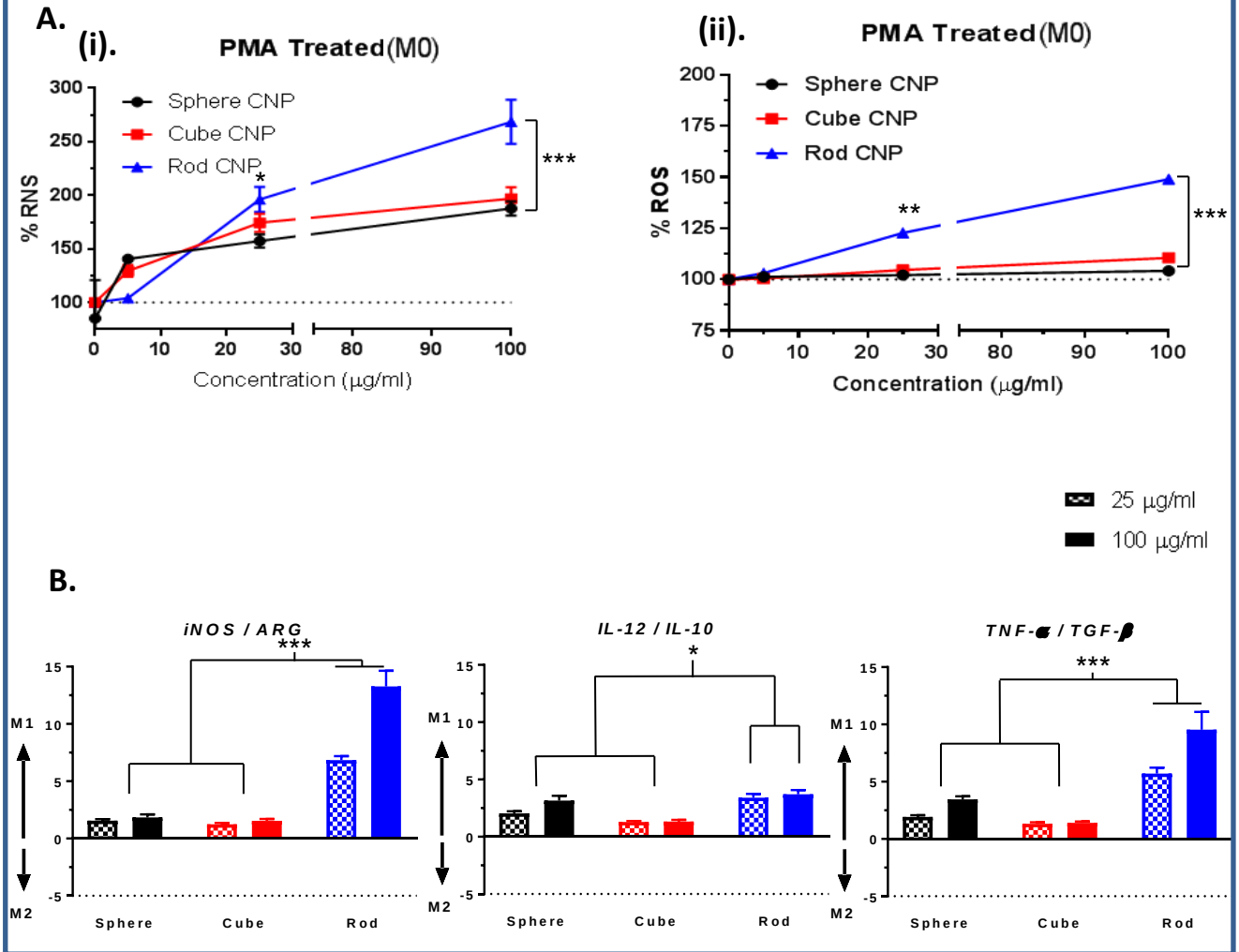

Figure 6: Priming capabilities of CNPs in naïve (M0) macrophages

A) Free radical (ROS/RNS) levels measured in naïve macrophages following CNP treatment (5, 25, 100µg/mL) (i) RNS (ii) ROS (n=6, two independent experiments). Untreated M0 cells were considered as control (depicted as 100%). Each CNP shape increased the free radical levels. However, Rod CNPs displayed a significant rise compared to Sphere and Cube CNPs. Data represented as mean ± SD.

B) M1/M2 ratio of gene expression of three pairs of mRNA markers (i) *iNOS/Arginase*, (ii) *IL-12/ IL-10* (iii) and *TNF-α/ TGF-β* expressed as fold change. Untreated M0 cells acted as control (n=4, two independent experiments). The M1/M2 ratio of mRNA expression in each pair was significantly higher at both concentrations (25 and 100µg/mL) in Rod CNPs compared to the other two shapes. Rod CNPs thus show promise in priming and activation of naïve macrophages without using any cytokines as stimuli. Data represented as mean ± SEM; *indicates $p < 0.05$, ** $p < 0.001$, *** $p < 0.0005$. Statistical significance by two-way ANOVA and Tukey post hoc test.

Positive M1/M2 ratio (positive y-axis) signifies higher M1 and lower M2 marker expression suggesting pre-dominant M1-like macrophages while negative M1/M2 ratio (negative Y-axis) denotes reduced M1 and elevated M2 marker expression, suggesting predominant population of alternately activated M2 macrophages. Since lower CNP dose (5μg/mL) of all three CNP shapes did not show much change in the macrophage phenotypes, we have not shown mRNA expression data (M1/M2 ratio) for 5μg/mL CNP dose.

The RNS levels were significantly higher for Sphere and Cube CNPs than the corresponding untreated control, which appeared to have minimal consequential effect on macrophage phenotype as measured by the mRNA expression (M1/M2 ratio<2-3 folds) (**Figure 6B**).

Rod CNPs consistently showed higher expression of M1 markers while suppressing M2 marker expression resulting in over 5-10 fold change in M1/M2 ratios (Blue bars, **Figure 6B**). The significant differences in M1 and M2 markers expression as evidenced by M1/M2 ratio were most prominent in *iNOS/Arginase* markers. Nitric oxide synthase (NOS) enzyme is responsible for arginine metabolism resulting in increased production of nitric oxide (indicative of RNS). The free radical modulation properties of CNPs and the subsequent macrophage phenotype corroborate the relation between *iNOS* and reactive nitrogen species[99]. Elevated levels of the free radicals and the upregulation of the M1 marker expression provided an early indication that free radical levels and macrophage phenotypes may be mechanistically linked.

The overall trend in terms of shape vs. macrophage priming set Rod CNPs distinctly apart from the other two shapes. Although the levels of free radicals were upregulated in all shapes, only Rod CNPs were capable of priming the macrophages towards M1-like phenotype. Other metallic NPs like gold (Au NPs) and silver (Ag NPs) have shown similar results *in vitro*[100, 101, 102, 103]. However, as exposure time increased beyond 3 h (Au NPs) [101, 102, 103] and 6 h (Ag NPs) [100, 101], the pro-

inflammatory response diminished as evidenced by respective gene expression. In contrast, in our study, CNPs exhibited sustained upregulation of pro-inflammatory M1 markers after 12 h of treatment that was sustained further after 24 h treatment as evidenced by insignificant decrease in the M1/M2 gene expression ratios (data not shown).

Metal oxides other than CNPs have also garnered attention for their macrophage priming effects. Zinc oxide (ZnO), Titanium dioxide (TiO_2) and Ag are the three major metal oxides studied so far. The extent of fold change in pro-M1 mRNA markers such as IL-6 and IL-1β in these studies ranged from 1.2 to 2[104]. In our study, both Sphere and Rod CNPs showed higher M1/M2 ratios (2-3 fold) in gene expression with Rod CNPs exhibiting much higher (8-10 fold) changes. Thus, CNPs demonstrated sustained activity in priming and activating macrophages. However, it should be noted that use of different cell line models and NP doses used in all these studies does not allow direct comparison among them.

3.5 Re-education of Macrophages

The use of NPs for the purpose of re-educating has been explored; however, the results have been far from encouraging. The ability of manipulating the microenvironmental cues to modulate the phenotype and consequently, the function of macrophages can alter or even halt progression of various diseases. For example, the inflammatory status of the microenvironment plays a key role in dictating the macrophage phenotype and hence, offers a promising alternative for macrophage re-education. Thus, we explored the strategy of modulating free radicals (ROS/RNS) levels by CNPs in order to guide the macrophage polarization. In this study, we investigated effects of CNPs

on re-educating both, the pro- and anti-inflammatory M1 and M2 macrophage phenotypes, respectively.

For these studies, THP-1 cells were pre-differentiated into either M1 or M2 phenotypes using protocol #3. Each of M1 and M2 phenotypes were then treated with different shapes of CNPs at different doses (0, 5, 25, 100μg/mL) for 12 h as described in **Section 2.7**. ROS/RNS levels along with mRNA expression of M1 and M2 markers were then measured for CNP-treated M1 and M2 cells similar to that described previously for naïve macrophages. For M1 and M2 cells, their corresponding untreated phenotypes (0μg/mL CNPs) served as baseline controls for comparison. Such normalization enables distinction between the effects exerted by the CNPs and the prior stimuli (LPS+IFN-γ or IL-4+IL-13) encountered by the cells.

Sphere CNPs elevated the free radical levels of both ROS and RNS in the pre-differentiated M1 cells in a dose-dependent manner compared to the untreated M1 (black line, **Figure 7A**). The effect was more pronounced in RNS levels. The dose-dependent effects for Sphere CNPs on ROS/RNS levels were not reflected as significantly on the gene expression **(**black bars, **Figure 7B)**. M1/M2 ratios indicated the propensity of Sphere CNPs to sustain the pro-inflammatory M1 phenotype of the pre-differentiated M1 macrophages.

Interestingly, Cube CNPs presented a mixed outcome in pre-differentiated M1 cells based on the dose used. At lower doses up to 25μg/mL, Cube scavenged free radicals driving the ROS/RNS levels below the baseline control (untreated M1 macrophages, dotted line, **Figure 7A**). At 100μg/mL dose, Cube CNPs exhibited pro-oxidant effect significantly increasing the ROS/RNS levels above the baseline controls (red lines, **Figure 7A**).

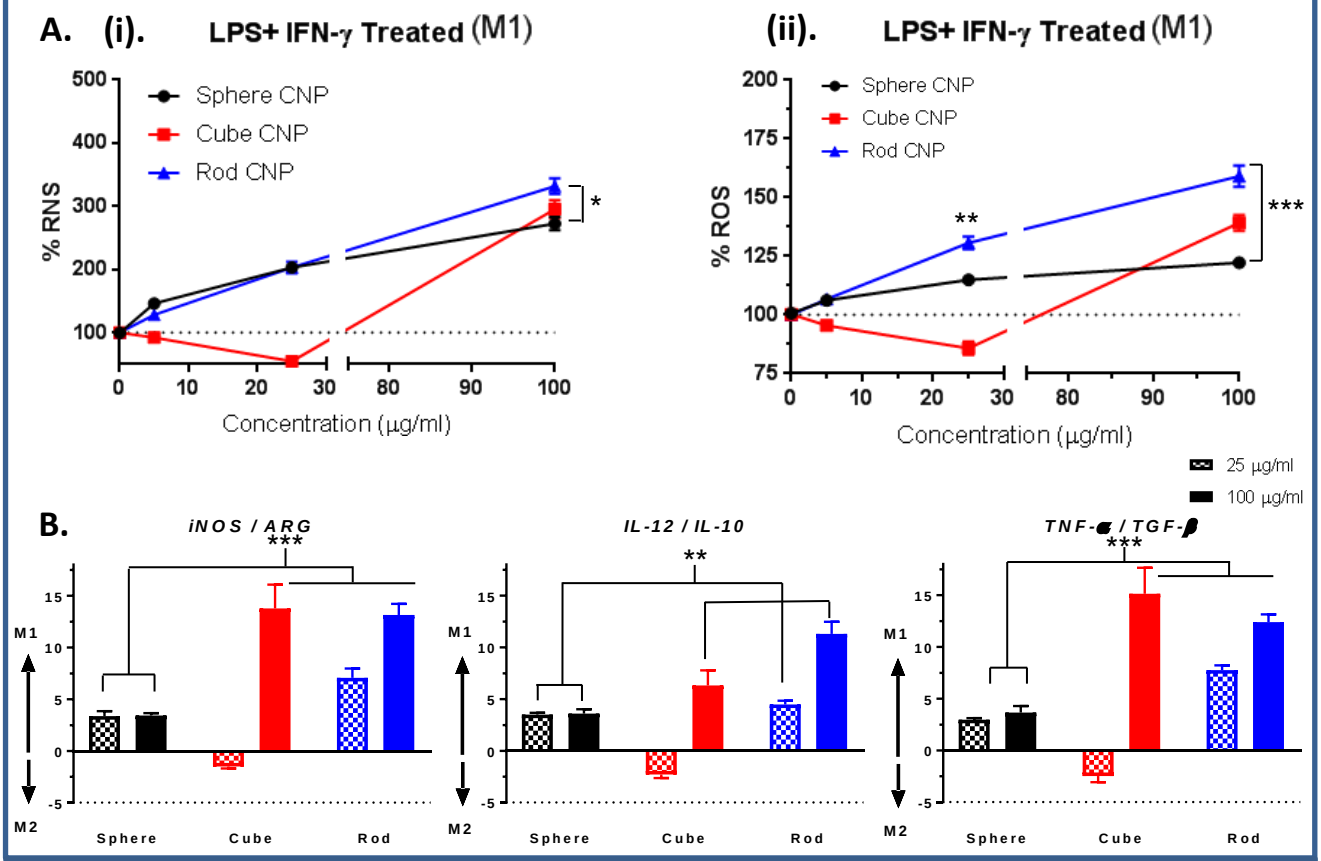

Figure 7: Effect of CNPs on pre-differentiated M1 macrophage phenotype

A) Free radical levels measured in pre-differentiated M1 macrophages following CNP treatment (5, 25, 100µg/mL) (i) RNS (ii) ROS (n=6, two independent experiments). Untreated M1 macrophages were considered as baseline control (depicted as 100%). The Sphere and Rod CNPs showed dose-dependent increase in the ROS/RNS levels compared to untreated M1 cell while Cube CNPs displayed decreased ROS/RNS below baseline levels at 25µg/mL, with increase at higher dose of 100µg/mL. Data represented as mean ± SD.

B) M1/M2 (M1>M2, plotted as positive Y-axis) or M2/M1 (M2>M1, plotted as negative Y-axis) ratio of fold change. Untreated M1 cells acted as control (n=4, two independent experiments). At higher dose, Rod and Cube significantly upregulated M1 markers compared to Sphere CNPs. Cube CNPs displayed peculiar divergent effects on the macrophage phenotype where low CNP dose (25µg/mL) resulted in anti-inflammatory M2-like phenotype and higher dose (100µg/mL) favored the pro-inflammatory M1 phenotype. Data represented as mean ± SEM; *indicates $p < 0.05$, ** $p < 0.001$, *** $p < 0.0005$. Statistical significance by two-way ANOVA and Tukey post hoc test.

Similar to the switch in anti-oxidant (25μg/mL) and pro-oxidant behavior (100μg/mL), we also observed switch in the macrophage phenotype in M1 and M2 macrophages treated with Cube CNPs (red bars, **Figure 7B)**. The M1/M2 expression ratios for all three pairs of M1 and M2 markers indicated a predominant M2 phenotype at 25μg/mL Cube CNP dose, supporting observed anti-oxidant effect (red lines, **Figure 7A)** while at 100μg/mL dose, the M1/M2 ratios exhibited predominant M1-like phenotype supporting pro-oxidant effect observed at this dose (red lines, **Figure 7A** and filled red bars, **Figure 7B**). The pre-dominant M2 phenotype observed in these Cube CNP-treated M1 macrophages was most pronounced in IL-12/IL-10 ratio implying the role of pro- and anti-inflammatory cytokines, respectively.

When pre-differentiated M1 macrophages were treated with Rod CNPs, the ROS levels were elevated to the highest levels amongst all shapes with RNS levels similar to the Sphere and Cube CNPs. The M1/M2 ratios for Rod CNPs across all pairs also exhibited M1-like phenotype, the magnitude of which was dose-dependent. The M1/M2 ratios for all three pairs showed 10-fold higher M1 marker expression at 100μg/mL dose of Rod CNPs (blue bars, **Figure 7B**).

In the pre-differentiated M2 cells, Sphere CNPs reduced the free radical levels below those observed in untreated M2 macrophages **(**black line, **Figure 8A)**. Significantly higher ROS/RNS levels compared to untreated M2 macrophages signified the pro-oxidant effects of Cube CNPs (red line, **Figure 8A)**. The magnitude of ROS/RNS levels was higher in Cube CNPs compared to other shapes in pre-differentiated M2 cells **(**red line, **Figure 8A)**. Rod CNPs displayed trend similar to Cube CNPs, elevating the ROS/RNS levels. The RNS levels were significantly lower in Rod CNPs than Cube CNPs yet the overall effect was pro-oxidant in nature **(**blue line, **Figure 8A)**.

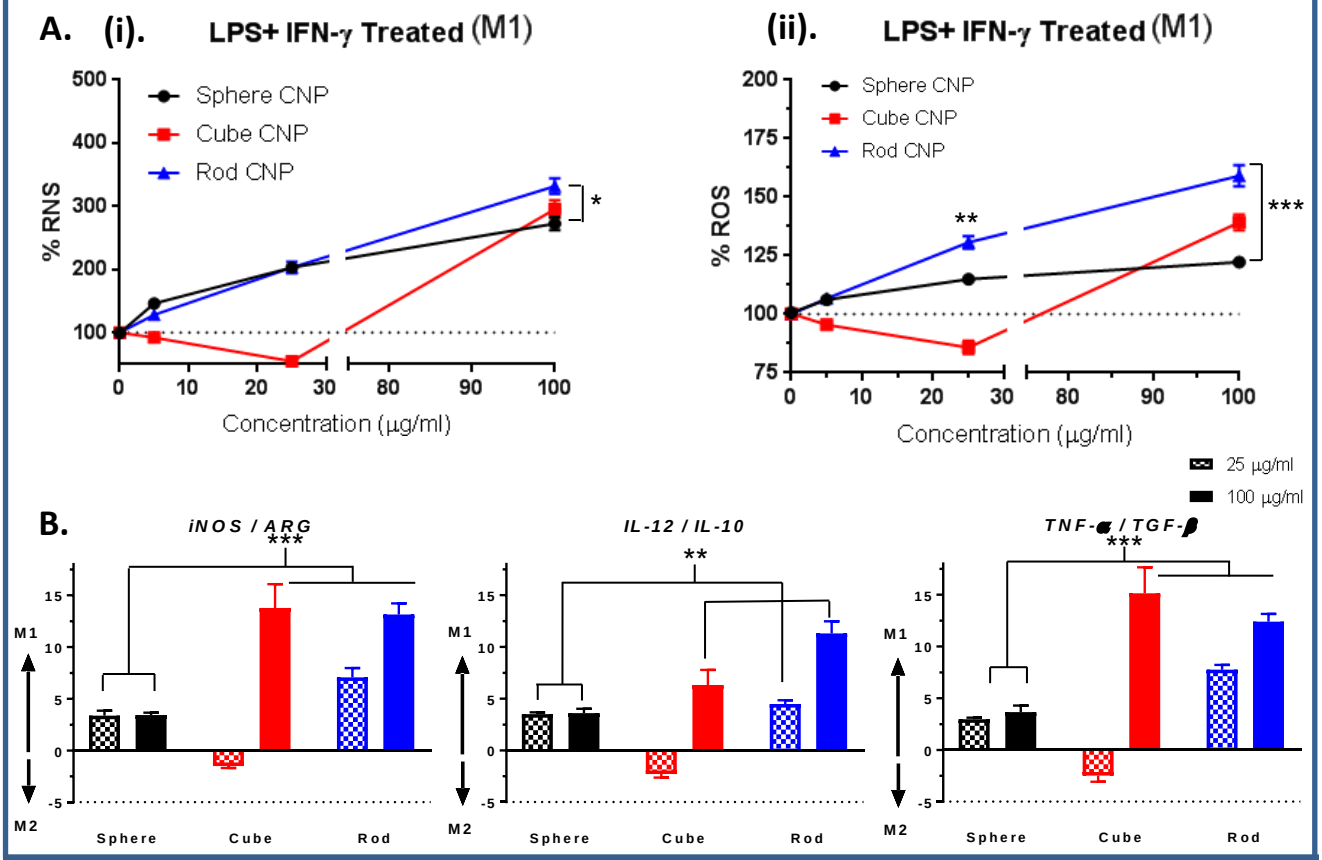

Figure 8: Effect of CNPs on pre-differentiated M2 macrophage phenotype

A) Free radical levels measured in pre-differentiated M2 macrophages following CNP treatment (5, 25, 100μg/mL) (i) RNS (ii) ROS (n=6, two independent experiments). Untreated M2 macrophages were considered as baseline control (depicted as 100%). Sphere CNPs decreased free radical levels compared to untreated M2 cells, while Cube and Rod CNPs exhibited a pro-inflammatory effect. Data represented as mean ± SD.

B) M1/M2 (M1>M2, plotted as positive Y-axis) or M2/M1 (M2>M1, plotted as negative Y-axis) ratio of fold change. Untreated M2 cells acted as control (n=4, two independent experiments). Rod CNPs were most effective in directing the cells towards M1-like phenotype followed by Cube CNPs. Sphere CNPs, on the other hand, maintained the anti-inflammatory M2-like phenotype. Data represented as mean ± SEM; *indicates $p < 0.05$, ** $p < 0.001$, *** $p < 0.0005$, **** $p < 0.0001$. Statistical significance by two-way ANOVA and Tukey post hoc test.

The anti-inflammatory response of Sphere CNPs was also reflected in the M1/M2 expression ratio of all three pairs with the M1/M2 balance skewed towards the M2 phenotype (black bar, **Figure 8B**). Sphere was the only shape out of the three to show such M2-like outcome. The Cube CNPs, on the other hand, displayed a re-programming effect on pre-differentiated M2 macrophages at all

concentrations. The M1/M2 expression ratios showed significantly higher (4-6) fold changes indicating higher M1 gene expression (red bars, **Figure 8B**). The re-programming effect of Rod CNPs was significantly higher (20-35 fold) than Cube CNPs especially at higher doses **(**blue bars, **Figure 8B)**.

The overall effect of Sphere CNP was limited to maintaining and slightly amplifying the pre-existing polarization state (M1 remained M1 and M2 remained M2). In other words, Sphere CNPs were able to maintain the status quo of the cells without drastically changing their phenotypes. Cube CNPs displayed mixed dose-dependent effects driving either M2-like or M1-like phenotypes in pre-differentiated M1 macrophages while they drove M1-like phenotype in pre-differentiated M2 macrophages. Rod CNPs showcased an overall drive towards M1-like phenotype in both pre-differentiated M1 and M2 macrophages.

To summarize, the results from Figures 6, 7, and 8 suggest that CNP shapes can maintain, modulate or drive pre-differentiated M0, M1 or M2 macrophages towards distinct phenotypes. The inherent nature of CNPs to boost the free radical levels was evident in all shapes, albeit to different degrees in pre-differentiated M1 cells. The anti- or pro-oxidant divergent effects were prominent in pre-differentiated M2 cells depending on the CNP shape. It was observed that some shapes have higher propensity to re-program (Rod CNPs), while others re-program pre-differentiated macrophage phenotypes only above a certain concentration threshold (e.g. Cube CNPs). Sphere was the least effective shape in terms of modulating the free radical balance and thus, influencing the macrophage phenotype. Although not effective in either priming or re-programming, their ability to boost the pre-existing phenotype could be used to supplement effects of the other shapes as well as other therapeutic interventions. Such supportive/supplemental role of Sphere CNPs needs further investigation. Cube and Rod CNPs, on the other hand, are both able to re-program the M2

macrophages into M1 macrophages as well as effectively maintain the pro-inflammatory M1 phenotype in pre-differentiated M1 macrophages.

Our results are interesting because many of the metal and metal oxide NPs investigated for their priming as well as re-programming capabilities did not exhibit both these actions together. This might be attributed to different signaling pathways controlling priming and re-programming effects. NPs with priming abilities alone have no effect on the pre-differentiated macrophages and may not be effective in halting the progression of the disease[28]. On the other hand, NPs capable of only re-programming may lose their effectiveness once macrophages start proliferating[20]. CNPs appear to have a pro-inflammatory effect on macrophages irrespective of their pre-existing polarization state. CNPs, thus, may have a potential to prime naïve macrophages. Our results also suggest that different shapes of CNPs can re-program already committed M1 or M2 macrophages towards a different macrophage phenotype. This strong influence on M0, M1 and M2 phenotypes sets CNPs apart from other NPs and shows their potential for re-programing, for example, predominantly M2 macrophages present in the tumor microenvironment towards tumor killing M1 macrophages.

3.6 Link between Free Radical Modulation and Macrophage Phenotype

All the results discussed so far, have displayed M1-like phenotypic characteristics when the inflammatory free radicals were upregulated. Similarly, scavenging free radicals led to an anti-inflammatory environment driving the M2-like phenotype. The priming and re-programming outcomes discussed previously, thus displayed a correlation between the inflammatory status of the microenvironment and the macrophage phenotype. Modulation of the free radical balance

using anti-oxidant therapy has been known to affect the macrophage phenotypes[105]. Anti-oxidant treatment prior to CNP administration could potentially decouple the interplay amongst the inflammatory microenvironment, macrophage polarization state, and CNP shape effects. The pre-differentiated M1 and M2 macrophages were treated with the anti-oxidant (N-acetyl cysteine, NAC, 1μM) prior to the treatment with Rod and Cube CNPs. Anti-oxidant NAC treatment alone (without CNPs) decreased ROS levels as expected and resulted in M2-like phenotype (**Figure 9A, B**).

As discussed previously, Cube and Rod CNPs have displayed tendency to induce M1-like phenotype. However, pre-treatment of M1 and M2 macrophages with anti-oxidant therapy resulted in different outcomes for the two CNP shapes. Cube CNPs could not overcome the anti-oxidant effects of NAC driving M2-like phenotype in both pre-differentiated M1 and M2 macrophages (red bars, **Figure 9A, B**). In contrast, Rod CNPs maintained higher levels of ROS even in the presence of NAC, maintaining the pro-inflammatory M1 phenotype. Although the M1/M2 ratio was considerably lower in NAC-pretreated Rod CNP treatment group, Rod CNPs retained their re-programming ability (blue bars, **Figure 9A, B**). The other interesting finding was the link between the free radical (ROS) levels and the macrophage polarization state. Our results suggest that control over the ROS levels can be exploited to guide or drive macrophage phenotype. Thus, CNP's ability of priming and re-programming macrophages can be attributed to their free radical modulation properties. Thus, CNP's ability of priming and re-programming macrophages can be attributed to their free radical modulation properties.

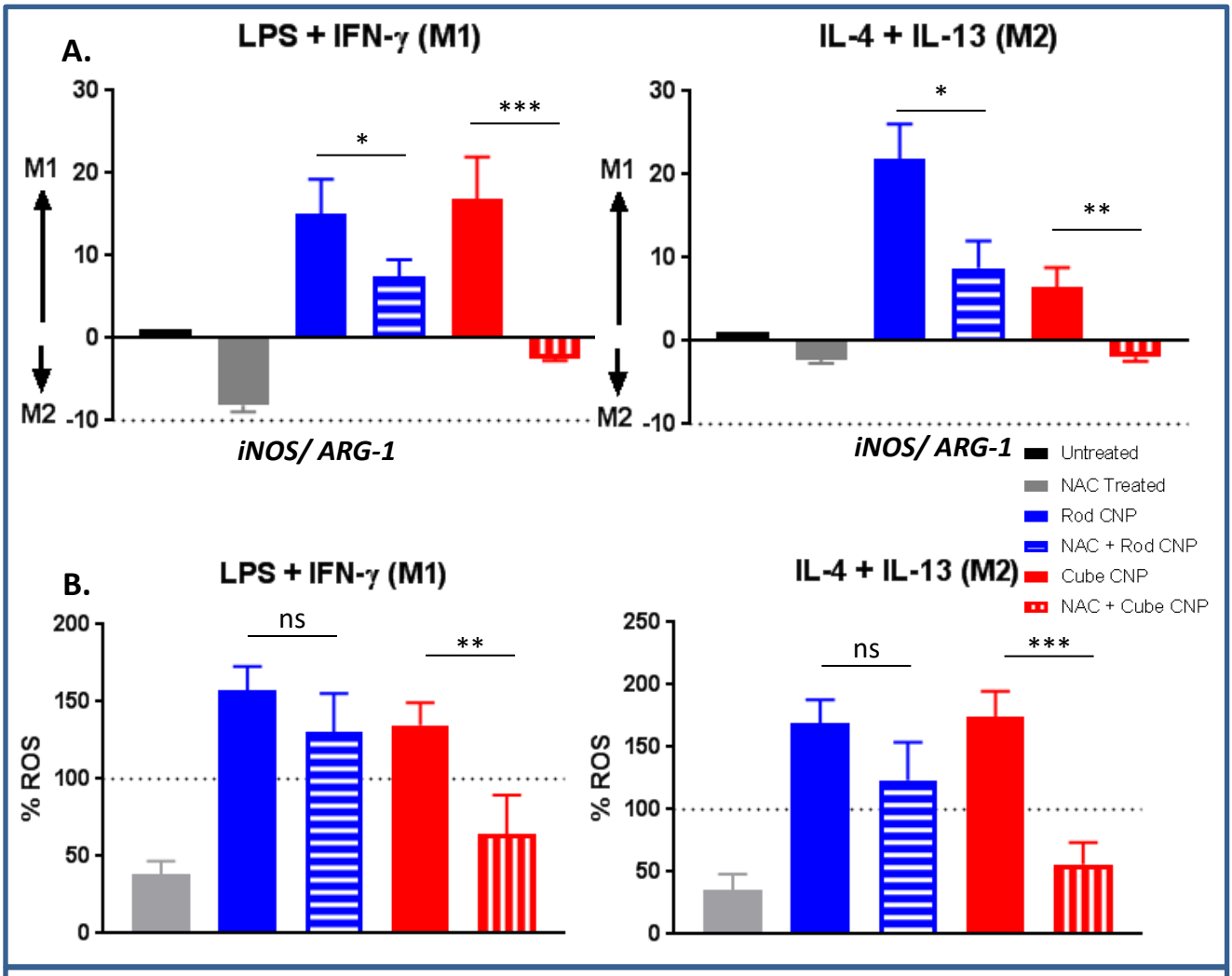

Figure 9: Anti-oxidant treatment modulating effect of CNPs on macrophage phenotype

A) M1/M2 (M1>M2, plotted on positive Y-axis) or M2/M1 ratio (M2>M1, plotted as negative Y-axis) was ratio measured for *iNOS/ Arginase* after antioxidant NAC pre-treatment followed by either Rod or Cube CNP administration. Untreated M1 and M2 macrophages without NAC and CNP treatment served as a baseline control. NAC- treated M1 and M2 macrophages without CNP treatment were considered as respective negative controls (n=4, two independent experiments). Rod CNPs (blue bars) maintained M1-like phenotype even in the presence of NAC in both, pre-differentiated M1 and M2 macrophages. On the other hand, in presence of NAC, Cube CNPs (red bars) could not maintain the M1-like phenotype. Data represented as mean ± SEM.

B) Free radical levels (% ROS) were measured in pre-differentiated M1 and M2 macrophages (n=4, two independent experiments). Pre-differentiated M1 and M2 macrophages were considered as baseline (100%). The pro-oxidant effect observed in Rod CNPs even after NAC treatment correlated with M1-like phenotype while the Cube CNPs could not overcome the anti-oxidant effects of NAC resulting in a M2-like phenotype. Data represented as mean ± SD; *indicates $p < 0.05$, ** $p < 0.001$, *** $p < 0.0005$. Statistical significance by one-way ANOVA and Tukey post hoc test.

Next, we probed the effects of a nitric oxide synthase (NOS) inhibitor, L-NAME on the macrophage phenotype and RNS levels in the pre-differentiated M1 and M2 macrophages. The enzymatic activity of NOS results in arginine metabolism producing nitric oxide. Inhibiting the pro-inflammatory arm of arginine metabolism by L-NAME naturally skewed the balance towards anti-inflammatory phenotype M2 in both, Cube and Rod CNP-treated M1 and M2 macrophages (**Figure 10A**). Treatment with L-NAME prior to CNP treatment significantly inhibited RNS production compared to respective untreated L-NAME control, Cube CNP group showing much higher inhibition than Rod CNP group. However, it was noticed that the L-NAME was not able to completely inhibit RNS production in Rod CNPs, leading to higher than baseline RNS levels **(**lined bars, **Figure 10B).**

The results imply that inhibition of iNOS abolished ability of both; Cube and Rod CNPs to drive M1-like macrophage phenotype in pre-differentiated M1 and M2 macrophages. However, surprisingly, CNPs, especially Rod CNPs, still produced higher RNS levels than baseline untreated macrophages.

ROS and nitric oxide (indicative of RNS) production by NADPH oxidase and iNOS, respectively is key to the anti-microbial activity of M1 macrophages[106]. The redox activity of CNPs has been well documented in the literature. Our results also suggested that the different CNP shapes play a role in guiding macrophage polarization as evident from the differential M1/M2 ratios of gene expression. The treatments with the anti-oxidant NAC and NOS inhibitor L-NAME were able to abolish such macrophage re-programming effects of CNPs suggesting that the ROS/RNS-rich microenvironment generated by CNPs also played role in macrophage re-programming.

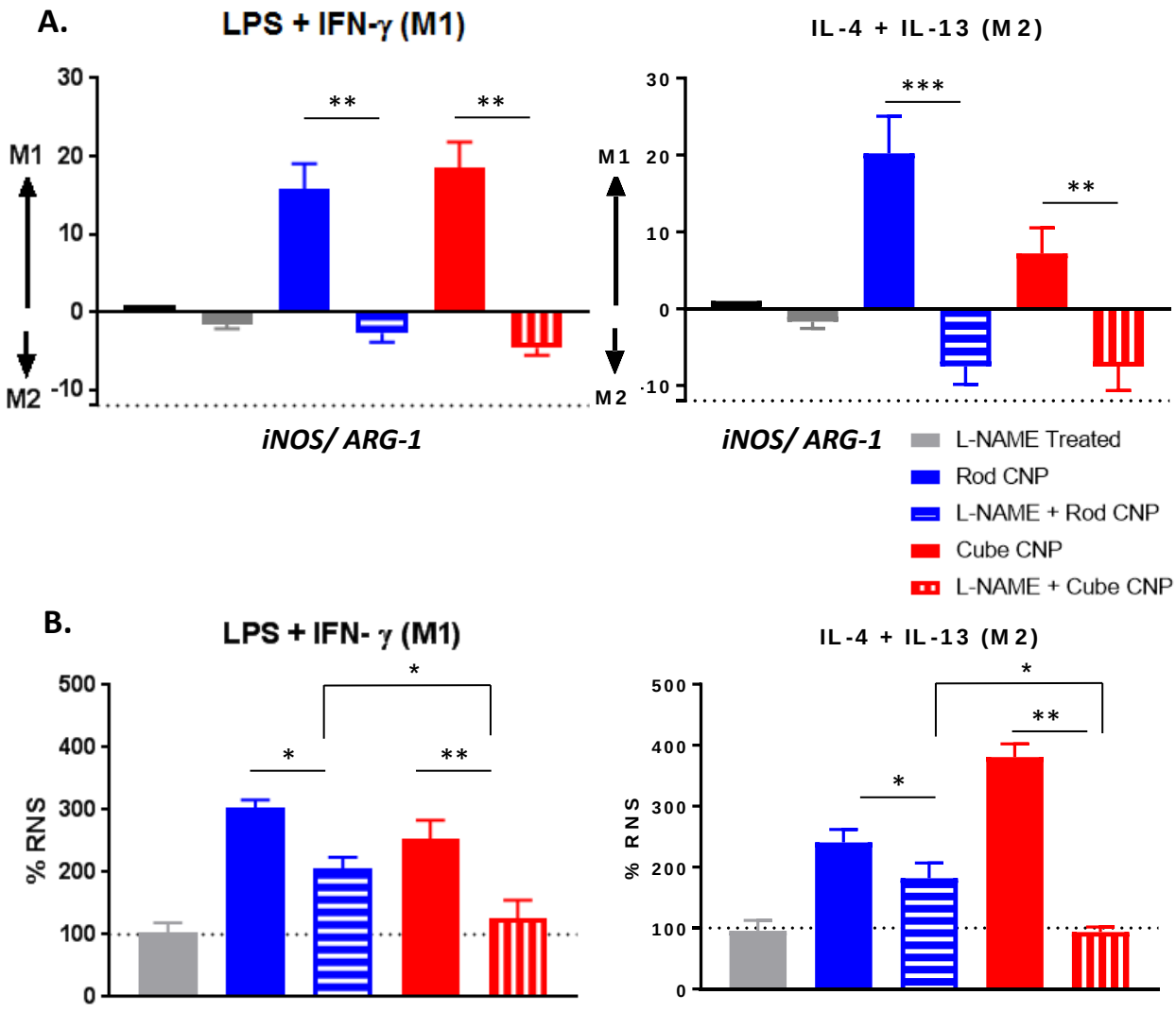

Figure 10: NOS inhibitor treatment modulating inflammatory conditions

A) M1/M2 (M1>M2, plotted on positive Y-axis) or M2/M1 ratio (M2>M1, plotted as negative Y-axis) was measured for of *iNOS/ Arginase* after L-NAME pre-treatment followed by either Rod or Cube CNP administration. Untreated M1 and M2 macrophages without NAC and CNP treatment served as baseline controls. L-NAME treated M1 and M2 cells without CNP treatment were considered as respective negative controls (n=4, two independent experiments). In all the L-NAME pre-treatment groups, arginase expression was predominantly higher than *iNOS* in both, Cube and Rod CNPs. Data are represented as mean ± SEM.

B) Free radical levels (% RNS) were measured in pre-differentiated M1 and M2 cells (n=4, two independent experiments). Pre-differentiated M1 and M2 macrophages were considered as baseline (100%). Pro-inflammatory effect (higher RNS levels than baseline) was observed in both, Cube and Rod CNPs although the effect was significantly reduced after L-NAME treatment. Data represented as mean ± SD; *indicates $p < 0.05$, ** $p < 0.001$, *** $p < 0.0005$. Statistical significance by one-way ANOVA and Tukey post hoc test.

The studies reported in this thesis have not elucidated the molecular mechanisms underlying the observed effects of different CNP shapes on ROS/RNS microenvironment and macrophage polarization. However, the encouraging results displayed by CNPs in macrophage activation provides viable alternative for newer and innovative immunotherapeutic approaches.

4.0 CONCLUSIONS AND FUTURE DIRECTIONS

Many diseases progress through oxidative stress with ROS being a key mediator as a primary cause as well as implicated in consequent downstream pathways. Literature reports are indicative of the regenerative capability of CNPs as redox agents. The ability to self-regenerate the surface makes CNPs unique from other NPs. Broad spectrum catalytic free radical modulation, small size and prolonged retention in tissues position CNPs as nanomaterials capable of immune modulation. Hence, even a small dose of CNPs can be effective for longer duration before being cleared from the body. However, the health effects and especially the long-term effects of CNP exposure are not yet understood fully, with reports claiming their ability to function in both protective as well as toxic manner. Use of CNPs and by extension, any metallic NPs should thus be approached with caution.

Monocytes and differentiated macrophages are a heterogeneous group of cells pro-active throughout an immune response. Although recent immunotherapeutic research focuses more on adaptive immune system such as cytotoxic T-cells due to their high specificity and potency, macrophage polarization also plays a pivotal role in directing the immune cascade. Considering the importance of macrophage re-programming in dictating the balance of immune system and the pathological processes of related diseases, such as cancer and chronic inflammation, NPs could be the mainstay of immunotherapy.

In this dissertation, we selected well characterized THP-1 human monocytes as *in vitro* cell line model for studying macrophage polarization. The THP-1 cells resemble primary monocytes and macrophages in morphological and functional properties including differentiation markers. The

first challenge was to reproducibly differentiate the monocytes to three different phenotypes; namely, M0, M1 and M2. The subsequent protocol developed in our lab recapitulates the different phenotypes as evidenced by their mRNA profiling. The naïve M0 macrophages displayed baseline levels of M1 and M2 markers. The M1 phenotype (LPS+IFN-γ treated) exhibited high expression levels of M1 markers (*iNOS, IL-12 and TNF-α*) and downregulation of M2 markers (*Arginase, IL-10 and TGF-β*). The M2 phenotype (IL-4+IL-13 treated) demonstrated exact opposite results with high expression of M2 markers and low expression of M1 markers.

We first investigated the priming potential of CNPs to drive naïve macrophages (M0) towards a particular phenotype without use of any cytokines or other stimulus. Rod CNPs emerged as a promising candidate to induce a pro-inflammatory character in these naïve cells prompting an M1-like response. Next, we explored the re-programming or re-educating capabilities of the CNPs in pre-differentiated M1 and M2 macrophages. In pre-differentiated M1 macrophages, all CNP shapes maintained and further boosted the free radical levels as compared to their corresponding untreated controls. The mRNA expression was also pre-dominantly maintained as M1-like. In pre-differentiated M2 cells, treatment with Sphere CNPs was ineffective in switching the polarization towards M1 phenotype. The anisotropic shapes such as Cube and Rod CNPs however, showed promise in terms of tilting the balance towards the pro-inflammatory M1 phenotype. The different aspect ratios of the three shapes as well as differences in isotropic properties indicate role of shape as a key biophysical factor dictating the macrophage response.

Further the similarities between the inflammatory status (ROS/RNS levels) of the environment surrounding the macrophages and their subsequent polarization state indicates an underlying connection between the two. Modulation of ROS/RNS levels as a tool to engineer and guide the macrophage polarization is a novel immunological approach.

Although THP-1 cell line acts as good model, it has limitations in mimicking the *in vivo* conditions. Relevant interaction between the target cells and their surrounding cells in their natural tissues in diseased condition is not captured in this set up. However, we have shown that CNPs have the initial promise and ability to guide or drive the polarization status of macrophages. Use of CNPs as an active carrier material for cytokine delivery could substantially reduce their dose without compromising on the effectiveness. Coupled with incorporation of biophysical characteristic like shape, regenerative properties and longer duration of action, CNPs could offer a viable alternative to existing immunotherapeutic approaches.

APPENDIX A

ABBREVIATIONS

Term	Abbreviation
NPs	Nanoparticles
CNPs	Cerium oxide NPs
NK	Natural killer cells
ROS	Reactive oxygen species
RNS	Reactive nitrogen species
iNOS	inducible Nitric oxide synthase
ARG	Arginase
IL	Interleukin
TGF-β	Transforming growth factor beta
TNF-α	Tumor necrosis factor alpha
LPS	Lipopolysaccharide
IFN-γ	Interferon gamma
NAC	N-acetyl cysteine

MDP	Muramyldipeptide
GM-CSF	Granulocyte-Macrophage Colony-stimulating Factor
RT-qPCR	Real Time Quantitative Polymerase Chain Reaction
MPS	Mononuclear Phagocytic System
TLR	Toll-like Receptor
TAMs	Tumor-associated Macrophages
PAMPs	Pathogen-associated microbial patterns
DAMPs	Danger-associated molecular patterns
SPIONs	Super paramagnetic iron-oxide NPs
SOD	Superoxide dismutase
TEM	Transmission Electron Microscope
PMA	Phorbol 12-myristate 13-acetate
PKC	Protein kinase C
DCFH-DA	2, 7-Dichlorodihydrofluorescein diacetate
DCF	2', 7'-Dichlorofluorescein
HBSS	Hank's Balanced Salt Solution
NED	N-1-napthylethylenediamine dihydrochloride
HLA	Human Leukocyte Antigen

PBS	Phosphate-buffered saline
L-NAME	L-N^G-Nitroarginine methyl ester
ANOVA	Analysis of Variance

BIBLIOGRAPHY

1. Janeway, C.A., Jr. & Medzhitov, R. Innate immune recognition. *Annu Rev Immunol* **20**, 197-216 (2002).

2. Laskin, D.L., Sunil, V.R., Gardner, C.R. & Laskin, J.D. Macrophages and Tissue Injury: Agents of Defense or Destruction? *Annu Rev Pharmacol* **51**, 267-288 (2011).

3. Wynn, T.A., Chawla, A. & Pollard, J.W. Macrophage biology in development, homeostasis and disease. *Nature* **496**, 445-455 (2013).

4. Kierdorf, K., Prinz, M., Geissmann, F. & Perdiguero, E.G. Development and function of tissue resident macrophages in mice. Seminars in immunology; 2015: Elsevier; 2015. p. 369-378.

5. Miao, X.Y., Leng, X.F. & Zhang, Q. The Current State of Nanoparticle-Induced Macrophage Polarization and Reprogramming Research. *Int J Mol Sci* **18** (2017).

6. Laskin, D.L. Macrophages and Inflammatory Mediators in Chemical Toxicity: A Battle of Forces. *Chem Res Toxicol* **22**, 1376-1385 (2009).

7. Montero-Vega, M.T. The inflammatory process underlying atherosclerosis. *Critical Reviews™ in Immunology* **32** (2012).

8. Grivennikov, S.I. & Karin, M. Inflammation and oncogenesis: a vicious connection. *Current opinion in genetics & development* **20**, 65-71 (2010).

9. Mantovani, A., Sica, A. & Locati, M. Macrophage polarization comes of age. *Immunity* **23**, 344-346 (2005).

10. Biswas, S.K., Chittezhath, M., Shalova, I.N. & Lim, J.Y. Macrophage polarization and plasticity in health and disease. *Immunol Res* **53**, 11-24 (2012).

11. Gordon, S. Alternative activation of macrophages. *Nat Rev Immunol* **3**, 23-35 (2003).

12. Sica, A. & Mantovani, A. Macrophage plasticity and polarization: in vivo veritas. *The Journal of clinical investigation* **122**, 787-795 (2012).

13. Colin, S., Chinetti-Gbaguidi, G. & Staels, B. Macrophage phenotypes in atherosclerosis. *Immunological reviews* **262**, 153-166 (2014).

14. Qian, B.Z. & Pollard, J.W. Macrophage Diversity Enhances Tumor Progression and Metastasis. *Cell* **141**, 39-51 (2010).

15. Hanahan, D. & Coussens, L.M. Accessories to the Crime: Functions of Cells Recruited to the Tumor Microenvironment. *Cancer Cell* **21**, 309-322 (2012).

16. DeNardo, D., Andreu, P. & Coussens, L.M. Interactions between lymphocytes and myeloid cells regulate pro- versus anti-tumor immunity. *Cancer Metast Rev* **29**, 309-316 (2010).

17. Murray, P.J. & Wynn, T.A. Protective and pathogenic functions of macrophage subsets. *Nat Rev Immunol* **11**, 723-737 (2011).

18. Huang, S. *et al.* Immune-Response in Mice That Lack the Interferon-Gamma Receptor. *Science* **259**, 1742-1745 (1993).

19. Dalton, D.K. *et al.* Multiple Defects of Immune Cell-Function in Mice with Disrupted Interferon-Gamma Genes. *Science* **259**, 1739-1742 (1993).

20. Yen, H.J., Hsu, S.H. & Tsai, C.L. Cytotoxicity and Immunological Response of Gold and Silver Nanoparticles of Different Sizes. *Small* **5**, 1553-1561 (2009).

21. Uttara, B., Singh, A.V., Zamboni, P. & Mahajan, R.T. Oxidative Stress and Neurodegenerative Diseases: A Review of Upstream and Downstream Antioxidant Therapeutic Options. *Curr Neuropharmacol* **7**, 65-74 (2009).

22. Drew, B. & Leeuwenburgh, C. Aging and the role of reactive nitrogen species. *Ann Ny Acad Sci* **959**, 66-81 (2002).

23. Kaplan, J. Active Oxygen. *Nature* **159**, 673-673 (1947).

24. West, A.P., Shadel, G.S. & Ghosh, S. Mitochondria in innate immune responses. *Nat Rev Immunol* **11**, 389 (2011).

25. Valko, M. *et al.* Free radicals and antioxidants in normal physiological functions and human disease. *The international journal of biochemistry & cell biology* **39**, 44-84 (2007).

26. Murray, P.J. & Wynn, T.A. Obstacles and opportunities for understanding macrophage polarization. *J Leukocyte Biol* **89**, 557-563 (2011).

27. Janeway, C.A., Jr. Approaching the asymptote? Evolution and revolution in immunology. *Cold Spring Harb Symp Quant Biol* **54 Pt 1**, 1-13 (1989).

28. Glass, C.K. & Natoli, G. Molecular control of activation and priming in macrophages. *Nat Immunol* **17**, 26-33 (2016).

29. Delves, P.J., Martin, S.J., Burton, D.R. & Roitt, I.M. *Essential immunology*. John Wiley & Sons, 2017.

30. Christmas, P. Toll-like receptors: sensors that detect infection. *Nature Education* **3**, 85 (2010).

31. Xia, T. *et al.* Comparison of the mechanism of toxicity of zinc oxide and cerium oxide nanoparticles based on dissolution and oxidative stress properties. *Acs Nano* **2**, 2121-2134 (2008).

32. Kawai, T. & Akira, S. Toll-like Receptors and Their Crosstalk with Other Innate Receptors in Infection and Immunity. *Immunity* **34**, 637-650 (2011).

33. Hennessy, E.J., Parker, A.E. & O'Neill, L.A.J. Targeting Toll-like receptors: emerging therapeutics? *Nat Rev Drug Discov* **9**, 293-307 (2010).

34. Lee, C.H., Kim, Y.J., Jang, J.H. & Park, J.W. Modulating macrophage polarization with divalent cations in nanostructured titanium implant surfaces. *Nanotechnology* **27** (2016).

35. Jain, S., Tran, T.H. & Amiji, M. Macrophage repolarization with targeted alginate nanoparticles containing IL-10 plasmid DNA for the treatment of experimental arthritis. *Biomaterials* **61**, 162-177 (2015).

36. Ito, A., Shinkai, M., Honda, H. & Kobayashi, T. Medical application of functionalized magnetic nanoparticles. *Journal of bioscience and bioengineering* **100**, 1-11 (2005).

37. Bernardini, G. *et al.* Toxicology of engineered metal nanoparticles. *General, applied and systems toxicology* (2009).

38. Petrarca, C. *et al.* Engineered metal based nanoparticles and innate immunity. *Clin Mol Allergy* **13**, 13 (2015).

39. Hussain, S. & Garantziotis, S. Interplay between apoptotic and autophagy pathways after exposure to cerium dioxide nanoparticles in human monocytes. *Autophagy* **9**, 101-103 (2013).

40. Chatterjee, S., Sarkar, S. & Bhattacharya, S. Toxic Metals and Autophagy. *Chem Res Toxicol* **27**, 1887-1900 (2014).

41. Di Gioacchino, M. *et al.* Autophagy as an ultrastructural marker of heavy metal toxicity in human cord blood hematopoietic stem cells. *Sci Total Environ* **392**, 50-58 (2008).

42. Roy, R. *et al.* Zinc oxide nanoparticles induce apoptosis by enhancement of autophagy via PI3K/Akt/mTOR inhibition. *Toxicol Lett* **227**, 29-40 (2014).

43. Marino, G., Niso-Santano, M., Baehrecke, E.H. & Kroemer, G. Self-consumption: the interplay of autophagy and apoptosis. *Nat Rev Mol Cell Bio* **15**, 81-94 (2014).

44. Bhattacharya, A., Prakash, Y.S. & Eissa, N.T. Secretory function of autophagy in innate immune cells. *Cell Microbiol* **16**, 1637-1645 (2014).

45. Zhang, Q. *et al.* Lysosomes involved in the cellular toxicity of nano-alumina: combined effects of particle size and chemical composition. *J Biol Regul Homeost Agents* **27**, 365-375 (2013).

46. Petrarca, C. *et al.* Palladium nanoparticles induce disturbances in cell cycle entry and progression of peripheral blood mononuclear cells: paramount role of ions. *J Immunol Res* **2014**, 295092 (2014).

47. Gornati, R. *et al. In vivo and in vitro models for nanotoxicology testing*. John Wiley and Sons: Chichester, 2009.

48. Frohlich, E. The role of surface charge in cellular uptake and cytotoxicity of medical nanoparticles. *Int J Nanomed* **7**, 5577-5591 (2012).

49. Bhattacharjee, S. *et al.* Cytotoxicity and cellular uptake of tri-block copolymer nanoparticles with different size and surface characteristics. *Part Fibre Toxicol* **9** (2012).

50. Champion, J.A. & Mitragotri, S. Role of target geometry in phagocytosis. *P Natl Acad Sci USA* **103**, 4930-4934 (2006).

51. Webb, S. Injecting nanoparticles into immunotherapy. *BioTechniques* **63**, 7-13 (2017).

52. Bruno, B.J., Miller, G.D. & Lim, C.S. Basics and recent advances in peptide and protein drug delivery. *Ther Deliv* **4**, 1443-1467 (2013).

53. Potnis, P.A., Dutta, D.K. & Wood, S.C. Toll-like receptor 4 signaling pathway mediates proinflammatory immune response to cobalt-alloy particles. *Cell Immunol* **282**, 53-65 (2013).

54. Monteiller, C. *et al.* The pro-inflammatory effects of low-toxicity low-solubility particles, nanoparticles and fine particles, on epithelial cells in vitro: the role of surface area. *Occup Environ Med* **64**, 609-615 (2007).

55. Peters, K. *et al.* Metallic nanoparticles exhibit paradoxical effects on oxidative stress and pro-inflammatory response in endothelial cells in vitro. *Int J Immunopath Ph* **20**, 685-695 (2007).

56. Moon, J.J., Huang, B. & Irvine, D.J. Engineering Nano- and Microparticles to Tune Immunity. *Adv Mater* **24**, 3724-3746 (2012).

57. Laskar, A., Eilertsen, J., Li, W. & Yuan, X.M. SPION primes THP1 derived M2 macrophages towards M1-like macrophages. *Biochem Bioph Res Co* **441**, 737-742 (2013).

58. Bartneck, M. *et al.* Peptide-Functionalized Gold Nanorods Increase Liver Injury in Hepatitis. *Acs Nano* **6**, 8767-8777 (2012).

59. Fuchs, A.K. *et al.* Carboxyl- and amino-functionalized polystyrene nanoparticles differentially affect the polarization profile of M1 and M2 macrophage subsets. *Biomaterials* **85**, 78-87 (2016).

60. Su, L. *et al.* Glycocalyx-Mimicking Nanoparticles for Stimulation and Polarization of Macrophages via Specific Interactions. *Small* **11**, 4191-4200 (2015).

61. Korsvik, C., Patil, S., Seal, S. & Self, W.T. Superoxide dismutase mimetic properties exhibited by vacancy engineered ceria nanoparticles. *Chem Commun*, 1056-1058 (2007).

62. Trovarelli, A. Catalytic properties of ceria and CeO2-containing materials. *Catal Rev* **38**, 439-520 (1996).

63. Sun, C.W., Li, H. & Chen, L.Q. Nanostructured ceria-based materials: synthesis, properties, and applications. *Energ Environ Sci* **5**, 8475-8505 (2012).

64. Pulido-Reyes, G. *et al.* Untangling the biological effects of cerium oxide nanoparticles: the role of surface valence states. *Sci Rep-Uk* **5**, 15613 (2015).

65. Culcasi, M. *et al.* EPR spin trapping evaluation of ROS production in human fibroblasts exposed to cerium oxide nanoparticles: evidence for NADPH oxidase and mitochondrial stimulation. *Chem-Biol Interact* **199**, 161-176 (2012).

66. Pesic, M. *et al.* Anti-cancer effects of cerium oxide nanoparticles and its intracellular redox activity. *Chem-Biol Interact* **232**, 85-93 (2015).

67. Lord, M.S. *et al.* Cellular uptake and reactive oxygen species modulation of cerium oxide nanoparticles in human monocyte cell line U937. *Biomaterials* **33**, 7915-7924 (2012).

68. Rosenkranz, P. *et al.* Effects of cerium oxide nanoparticles to fish and mammalian cell lines: An assessment of cytotoxicity and methodology. *Toxicol in Vitro* **26**, 888-896 (2012).

69. Deshpande, S., Patil, S., Kuchibhatla, S.V.N.T. & Seal, S. Size dependency variation in lattice parameter and valency states in nanocrystalline cerium oxide. *Appl Phys Lett* **87** (2005).

70. Karakoti, A., Singh, S., Dowding, J.M., Seal, S. & Self, W.T. Redox-active radical scavenging nanomaterials. *Chem Soc Rev* **39**, 4422-4432 (2010).

71. Ravishankar, T.N., Ramakrishnappa, T., Nagaraju, G. & Rajanaika, H. Synthesis and Characterization of CeO2 Nanoparticles via Solution Combustion Method for Photocatalytic and Antibacterial Activity Studies. *Chemistryopen* **4**, 146-154 (2015).

72. dos Santos, C.C.L. *et al.* Antimicrobial activity of nano cerium oxide (IV)(CeO2) against Streptococcus mutans. BMC proceedings; 2014: BioMed Central; 2014. p. P48.

73. Mai, H.X. *et al.* Shape-selective synthesis and oxygen storage behavior of ceria nanopolyhedra, nanorods, and nanocubes. *J Phys Chem B* **109**, 24380-24385 (2005).

74. Zhang, D.S. *et al.* Synthesis of CeO2 nanorods via ultrasonication assisted by polyethylene glycol. *Inorg Chem* **46**, 2446-2451 (2007).

75. Goel, G., Makkar, H.P., Francis, G. & Becker, K. Phorbol esters: structure, biological activity, and toxicity in animals. *International journal of toxicology* **26**, 279-288 (2007).

76. Park, E.K. *et al.* Optimized THP-1 differentiation is required for the detection of responses to weak stimuli. *Inflammation Research* **56**, 45-50 (2007).

77. Kigerl, K.A. *et al.* Identification of two distinct macrophage subsets with divergent effects causing either neurotoxicity or regeneration in the injured mouse spinal cord. *Journal of Neuroscience* **29**, 13435-13444 (2009).

78. Martinez, F.O., Helming, L. & Gordon, S. Alternative activation of macrophages: an immunologic functional perspective. *Annu Rev Immunol* **27**, 451-483 (2009).

79. Livak, K.J. & Schmittgen, T.D. Analysis of relative gene expression data using real-time quantitative PCR and the 2(T)(-Delta Delta C) method. *Methods* **25**, 402-408 (2001).

80. Bulger, E.M., Garcia, I. & Maier, R.V. Intracellular antioxidant activity is necessary to modulate the macrophage response to endotoxin. *Shock* **18**, 58-63 (2002).

81. Bon, C., Böhme, G.A., Doble, A., Stutzmann, J.M. & Blanchard, J.C. A Role for Nitric Oxide in Long-term Potentiation. *European Journal of Neuroscience* **4**, 420-424 (1992).

82. Xue, Y.F. *et al.* Shape-Specific Nanoceria Mitigate Oxidative Stress-Induced Calcification in Primary Human Valvular Interstitial Cell Culture. *Cell Mol Bioeng* **10**, 483-500 (2017).

83. Bosshart, H. & Heinzelmann, M. THP-1 cells as a model for human monocytes. *Ann Transl Med* **4**, 438 (2016).

84. Mariathasan, S. *et al.* Differential activation of the inflammasome by caspase-1 adaptors ASC and Ipaf. *Nature* **430**, 213-218 (2004).

85. Martinon, F., Burns, K. & Tschopp, J. The inflammasome: a molecular platform triggering activation of inflammatory caspases and processing of proIL-beta. *Mol Cell* **10**, 417-426 (2002).

86. Kovalovsky, D. *et al.* The Th1 and Th2 cytokines IFN-gamma and IL-4 antagonize the inhibition of monocyte IL-1 receptor antagonist by glucocorticoids: involvement of IL-1. *Eur J Immunol* **28**, 2075-2085 (1998).

87. Mantovani, A. *et al.* The chemokine system in diverse forms of macrophage activation and polarization. *Trends Immunol* **25**, 677-686 (2004).

88. Ahn, J.S. & Agrawal, B. IL-4 is more effective than IL-13 for in vitro differentiation of dendritic cells from peripheral blood mononuclear cells. *Int Immunol* **17**, 1337-1346 (2005).

89. Fenton, M., Vermeulen, M., Clark, B., Webb, A. & Auron, P. Human pro-IL-1 beta gene expression in monocytic cells is regulated by two distinct pathways. *The Journal of Immunology* **140**, 2267-2273 (1988).

90. Allavena, P., Sica, A., Garlanda, C. & Mantovani, A. The Yin-Yang of tumor-associated macrophages in neoplastic progression and immune surveillance. *Immunol Rev* **222**, 155-161 (2008).

91. Liu, Y. & Cao, X. The origin and function of tumor-associated macrophages. *Cell Mol Immunol* **12**, 1-4 (2015).

92. Martinez, F.O., Sica, A., Mantovani, A. & Locati, M. Macrophage activation and polarization. *Front Biosci-Landmrk* **13**, 453-461 (2008).

93. Sica, A. *et al.* Macrophage polarization in tumour progression. *Semin Cancer Biol* **18**, 349-355 (2008).

94. Lucarelli, M. *et al.* Innate defence functions of macrophages can be biased by nano-sized ceramic and metallic particles. *Eur Cytokine Netw* **15**, 339-346 (2004).

95. Tran, T.H., Rastogi, R., Shelke, J. & Amiji, M.M. Modulation of Macrophage Functional Polarity towards Anti-Inflammatory Phenotype with Plasmid DNA Delivery in CD44 Targeting Hyaluronic Acid Nanoparticles. *Sci Rep-Uk* **5** (2015).

96. Ma, J. *et al.* Crucial Role of Lateral Size for Graphene Oxide in Activating Macrophages and Stimulating Pro-inflammatory Responses in Cells and Animals. *Acs Nano* **9**, 10498-10515 (2015).

97. Verrecchia, F. & Mauviel, A. TGF-beta and TNF-alpha: antagonistic cytokines controlling type I collagen gene expression. *Cell Signal* **16**, 873-880 (2004).

98. Ma, X. *et al.* Regulation of IL-10 and IL-12 production and function in macrophages and dendritic cells. *F1000Res* **4** (2015).

99. Rath, M., Muller, I., Kropf, P., Closs, E.I. & Munder, M. Metabolism via Arginase or Nitric Oxide Synthase: Two Competing Arginine Pathways in Macrophages. *Front Immunol* **5**, 532 (2014).

100. Nishanth, R.P., Jyotsna, R.G., Schlager, J.J., Hussain, S.M. & Reddanna, P. Inflammatory responses of RAW 264.7 macrophages upon exposure to nanoparticles: Role of ROS-NF kappa B signaling pathway. *Nanotoxicology* **5**, 502-516 (2011).

101. Hashimoto, M. *et al.* Responses of RAW264.7 macrophages to water-dispersible gold and silver nanoparticles stabilized by metal-carbon sigma-bonds. *J Biomed Mater Res A* **102**, 1838-1849 (2014).

102. Bancos, S., Stevens, D.L. & Tyner, K.M. Effect of silica and gold nanoparticles on macrophage proliferation, activation markers, cytokine production, and phagocytosis in vitro. *Int J Nanomed* **10**, 183-206 (2015).

103. Zhang, Q., Hitchins, V.M., Schrand, A.M., Hussain, S.M. & Goering, P.L. Uptake of gold nanoparticles in murine macrophage cells without cytotoxicity or production of pro-inflammatory mediators. *Nanotoxicology* **5**, 284-295 (2011).

104. Giovanni, M. *et al.* Pro-inflammatory responses of RAW264.7 macrophages when treated with ultralow concentrations of silver, titanium dioxide, and zinc oxide nanoparticles. *J Hazard Mater* **297**, 146-152 (2015).

105. Covarrubias, A., Byles, V. & Horng, T. ROS sets the stage for macrophage differentiation. *Cell Res* **23**, 984-985 (2013).

106. Reuter, S., Gupta, S.C., Chaturvedi, M.M. & Aggarwal, B.B. Oxidative stress, inflammation, and cancer How are they linked? *Free Radical Bio Med* **49**, 1603-1616 (2010).